

1 **MIXv2: a long-term mosaic emission inventory for**  
2 **Asia (2010-2017)**

3  
4 **Meng Li<sup>1,2</sup>, Junichi Kurokawa<sup>3</sup>, Qiang Zhang<sup>4</sup>, Jung-Hun Woo<sup>5,6</sup>, Tazuko Morikawa<sup>7</sup>, Satoru**  
5 **Chatani<sup>8</sup>, Zifeng Lu<sup>9</sup>, Yu Song<sup>10</sup>, Guannan Geng<sup>11</sup>, Hanwen Hu<sup>11</sup>, Jinseok Kim<sup>6</sup>, Owen R. Cooper<sup>1,2</sup>,**  
6 **Brian C. McDonald<sup>2</sup>**

7 <sup>1</sup> Cooperative Institute for Research in Environmental Sciences, University of Colorado, Boulder, CO,  
8 USA

9 <sup>2</sup> NOAA Chemical Sciences Laboratory, Boulder, CO, USA

10 <sup>3</sup> Asia Center for Air Pollution Research, 1182 Sowa, Nishi-ku, Niigata, Niigata, 950-2144, Japan

11 <sup>4</sup> Ministry of Education Key Laboratory for Earth System Modeling, Department of Earth System  
12 Science, Tsinghua University, Beijing, China

13 <sup>5</sup> Department of Civil and Environmental Engineering, Konkuk University, Seoul, Republic of Korea

14 <sup>6</sup> Department of Technology Fusion Engineering, Konkuk University, Seoul, Republic of Korea

15 <sup>7</sup> Japan Automobile Research Institute, 2530 Karima, Tsukuba, Ibaraki, 305-0822, Japan

16 <sup>8</sup> National Institute for Environmental Studies, 16-2 Onogawa, Tsukuba, Ibaraki, 305-8506, Japan

17 <sup>9</sup> Energy Systems and Infrastructure Analysis Division, Argonne National Laboratory, Lemont, IL, USA

18 <sup>10</sup> State Key Joint Laboratory of Environmental Simulation and Pollution Control, Department of  
19 Environmental Science, Peking University, Beijing, People's Republic of China

20 <sup>11</sup> State Key Joint Laboratory of Environmental Simulation and Pollution Control, School of Environment,  
21 Tsinghua University, Beijing, China

22

23

24

25

26

27

28 *Correspondence to:* Meng Li (Meng.Li-1@colorado.edu)

29

30

Deleted: 100084

## 32 Abstract

33 The MIXv2 Asian emission inventory is developed under the framework of the Model Inter-  
34 Comparison Study for Asia (MICS-Asia) Phase IV, and produced from a mosaic of up-to-date  
35 regional emission inventories. We estimated the emissions for anthropogenic and biomass  
36 burning sources covering 23 countries and regions in East, Southeast and South Asia, and  
37 aggregated emissions to a uniform spatial and temporal resolution for seven sectors: power,  
38 industry, residential, transportation, agriculture, open biomass burning and shipping. Compared  
39 to MIXv1, we extended the dataset to 2010 – 2017, included emissions of open biomass burning  
40 and shipping, and provided model-ready emissions of SAPRC99, SAPRC07, and CB05. A series  
41 of unit-based point source information was incorporated covering power plants in China and  
42 India. A consistent speciation framework for Non-Methane Volatile Organic Compounds  
43 (NMVOCs) was applied to develop emissions by three chemical mechanisms. The total Asian  
44 emissions for anthropogenic | open biomass sectors in 2017 are estimated as follows: 41.6 | 1.1  
45 Tg NO<sub>x</sub>, 33.2 | 0.1 Tg SO<sub>2</sub>, 258.2 | 20.6 Tg CO, 61.8 | 8.2 Tg NMVOC, 28.3 | 0.3 Tg NH<sub>3</sub>, 24.0 |  
46 2.6 Tg PM<sub>10</sub>, 16.7 | 2.0 Tg PM<sub>2.5</sub>, 2.7 | 0.1 Tg BC, 5.3 | 0.9 Tg OC, and 18.0 | 0.4 Pg CO<sub>2</sub>. The  
47 contributions of India and Southeast Asia have been emerging in Asia during 2010-2017,  
48 especially for SO<sub>2</sub>, NH<sub>3</sub> and particulate matters. [Gridded emissions at a spatial resolution of 0.1  
49 degree with monthly variations are now publicly available. This updated long-term emission  
50 mosaic inventory is ready to facilitate air quality and climate model simulations, as well as  
51 policy-making and associated analyses.](#)

Deleted: at  
<https://cs1.noaa.gov/groups/cs14/modeldata/data/Li2023/>.

Deleted: ¶

## 53 1. Introduction

54 [Air pollutants emitted from both anthropogenic and natural activities have caused severe impacts  
55 on human health, ecosystems, and climate over Asia \(Adam et al., 2021; Geng et al., 2021;  
56 Takahashi et al., 2020; Wong et al., 2008; Xie et al., 2018\). Over the last two decades, the  
57 emerging ozone pollution and haze events across Asia have got extensive attention from the  
58 government \(Anwar et al., 2021; Feng et al., 2022; Zheng et al., 2018\). Tremendous efforts have  
59 been made since 2010 continuously to improve air quality and protect human health. The effects  
60 of these policies on emission abatement need to be updated in inventories, to address the regional  
61 and global issues of air quality and climate change. Therefore, a long-term emission inventory  
62 plays key roles in historical policy assessment, and future air quality and climate mitigation.](#)  
63 [Consistent greenhouse gas emissions are crucial for climate-air quality nexus research and  
64 policymaking \(Fiore et al., 2015\). Carbon dioxide \(CO<sub>2</sub>\) is co-emitted with many air pollutants  
65 which are contributors of ozone and particulate matter, further changing climate through forcings  
66 of Earth's radiation budget \(Fiore et al., 2015\). Previous studies have emphasized the importance  
67 of air pollution mitigation and climate change \(Jacob and Winner, 2009; Saari et al., 2015\), as  
68 recently summarized by the Synthesis Report of the IPCC Sixth Assessment Report \(IPCC:  
69 Intergovernmental Panel on Climate Change, report available at  
70 <https://www.ipcc.ch/report/sixth-assessment-report-cycle/>\). Given the common sources of CO<sub>2</sub>  
71 and air pollutants, it's important to quantify their emissions distribution in a self-consistent way](#)

75 to assess the co-benefits and pathways to cleaner air and carbon neutrality (Klausbrückner et al.,  
76 2016; Phillips, 2022; von Schneidmesser and Monks, 2013).

77 Emissions over Asia since 2010 are quantified in recent studies. Kurokawa et al. (2020)  
78 developed an anthropogenic emission inventory over Asia for 1950-2015, REAS (the Regional  
79 Emission inventory in ASia), covering power plants, industry, residential, transportation and  
80 agricultural sources. Emissions of both air pollutants and CO<sub>2</sub> are estimated in REAS. Based on  
81 the Community Emissions Data System (CEDS), McDuffie et al. (2020) developed a global  
82 anthropogenic emission inventory covering major air pollutants over 1970-2017. Global  
83 emissions for air pollutants are estimated under the HTAPv3 (Task Force on Hemispheric  
84 Transport of Air Pollution) project for 2000-2018 for air pollutants by integrating official  
85 inventories over specific areas including Asia (Crippa et al., 2023). These regional / global  
86 emissions are estimated with limited updates of country-specific or even localized information.  
87 Following a mosaic approach, the first version of MIX Asian inventory (MIXv1) was developed  
88 to support the Model Inter-Comparison Study for Asia (MICS-Asia) Phase III projects, by  
89 incorporating five regional emission inventories for all major anthropogenic sources over Asia,  
90 providing a gridded emission dataset at a spatial resolution of 0.25 degree for 2008 and 2010.  
91 The mosaic approach has been proved to increase the emission accuracy and model performance  
92 significantly by including more local information (Li et al., 2017c). A profile-based speciation  
93 scheme for Non-Methane Volatile Organic Compounds (NMVOCs) was applied to develop  
94 model-ready emissions by chemical mechanisms, which reduced the uncertainties arising from  
95 inaccurate mapping between inventory and model species (Li et al., 2014; Li et al., 2019b).  
96 Specifically, MIXv1 advances our understanding of emissions and spatial distributions from  
97 power plants through a mosaic of unit-based information, and agricultural activities based on a  
98 process-based model which parameterized the spatial and temporal variations of emission factors  
99 for NH<sub>3</sub>.

100 However, it's difficult to develop consistent emissions over Asia for a long period using the  
101 mosaic approach because of the lack of available regional inventory data. Within the MICS-Asia  
102 community, developers of regional inventories have been endeavoring to extend their emission  
103 inventories to the present day since Phase IV. Through intensive collaboration and community  
104 efforts, we now have a complete list of available regional emission inventories covering major  
105 parts of Asia, and are able to combine them to produce a new version of MIX for 2010-2017.  
106 MICS-Asia is currently in its fourth phase, MICS-Asia IV, which aims to advance our  
107 understanding of the discrepancies and relative uncertainties present in the simulations of air  
108 quality and climate models (Chen et al., 2019; Gao et al., 2018; Itahashi et al., 2020; Li et al.,  
109 2017c). A critical component of the project is ensuring that emission inventories remain  
110 consistent across various atmospheric and climate models. In support of MICS-Asia IV research  
111 activities and related policy-making endeavors, we developed MIXv2, the second version of our  
112 mosaic Asian inventory. MIXv2 combines the best available state-of-the-art regional emission  
113 inventories from across Asia using a mosaic approach. This inventory is expected to enhance our  
114 capabilities to assess emission changes and their driving forces, and their impact on air quality  
115 and climate change, thus providing valuable insights for decision-makers and stakeholders. CO<sub>2</sub>

**Moved (insertion) [1]**

**Deleted:** Tremendous efforts have been made continuously to improve air quality and protect human health in Asia since 2010, and these effects on emission abatement need to be updated in inventories (Zheng et al., 2018). In this regard, a long-term inventory with updated information is critical.

**Deleted:** Zheng et al., 2018). In this regard, a long-term inventory with updated information is critical.

**Deleted:** ). In this regard, a long-term inventory with updated information is critical.

**Deleted:**

126 emissions are estimated based on the same emission inventory framework as the short-lived air  
 127 pollutants, and further integrated into MIXv2 following the mosaic methodology.  
 128 MIXv1 has been widely applied to support scientific research activities from regional to local  
 129 scales (Geng et al., 2021; Hammer et al., 2020; Li et al., 2019a; Li et al., 2017c). Compared to  
 130 MIXv1, MIXv2 has the following updates to better feed the needs of atmospheric modelling  
 131 activities:  
 132 - advances the horizontal resolution of the gridded maps from 0.25 to 0.1 degree  
 133 - incorporates up-to-date regional inventories from 2010-2017  
 134 - provides emissions of open biomass burning and shipping, in addition to anthropogenic sources  
 135 - develops model-ready emissions of SAPRC99, SAPRC07 and CB05  
 136 Methods and input data are described in Sect. 2. Emissions evolution and their driving forces,  
 137 seasonality, spatial distribution, NMVOC speciation and inventory limitations are analyzed and  
 138 discussed in Sect. 3. Sect. 4 compares the MIX data with other bottom-up and top-down  
 139 emission estimates. Concluding remarks are provided in Sect. 5.  
 140

## 141 2. Methods and Inputs

### 142 2.1 Overview of MIXv2

143 The key features of MIXv2 are summarized in Table 1. Anthropogenic sources, including power,  
 144 industry, residential, transportation and agriculture, along with open biomass burning and  
 145 shipping are included. Dust and aviation are not included in the current version of MIX. Monthly  
 146 emissions between 2010 – 2017 are allocated to grids at 0.1 × 0.1 degree. Open biomass burning  
 147 emissions are also available with daily resolution. Emissions of ten species, including CO<sub>2</sub> and  
 148 air pollutants of NO<sub>x</sub>, SO<sub>2</sub>, CO, NMVOC, NH<sub>3</sub>, PM<sub>10</sub>, PM<sub>2.5</sub>, BC and OC are estimated. MIX  
 149 can support most atmospheric models compatible with gas-phase chemical mechanisms of  
 150 SAPRC99, SAPRC07, CB05, and those can be mapped based on these three chemical  
 151 mechanisms (e.g., GEOS-Chem, MOZART) (Li et al., 2014). As shown in Figure 1, MIXv2  
 152 stretches from Afghanistan in the west to Japan in the east, from Indonesia in the south to  
 153 Mongolia in the north. The domain is consistent with the REASv3 gridded emissions product.  
 154 Table 2 summarizes the subsectors for each sector in the development of MIX, along with the  
 155 corresponding source codes used by IPCC.  
 156

### 157 2.2 Mosaic Methodology

158 We follow a mosaic methodology similar to the development of MIXv1 (Li et al., 2017c), as shown  
 159 in Figure 1. In brief, nine regional and two global emission inventories were collected and  
 160 integrated into a uniform format, including: REAS version 3 for Asia (referred to as REASv3)

~~Deleted:~~ The Model Inter-Comparison Study for Asia (MICS-Asia) is a research project currently in its fourth phase, MICS-Asia IV, which aims to advance our understanding of the discrepancies and relative uncertainties present in the simulations of air quality and climate mo... [1]

~~Deleted:~~ Chen et al., 2019; Gao et al., 2018; Itahashi ... [2]

~~Deleted:~~ ; Gao et al., 2018; Itahashi et al., 2020; Li et ... [3]

~~Deleted:~~ Gao et al., 2018; Itahashi et al., 2020; Li et a... [4]

~~Deleted:~~ ; Itahashi et al., 2020; Li et al., 2017c). A cri... [5]

~~Deleted:~~ Itahashi et al., 2020; Li et al., 2017c). A criti... [6]

~~Deleted:~~ ; Li et al., 2017c). A critical component of th... [7]

~~Deleted:~~ Li et al., 2017c). A critical component of the... [8]

~~Deleted:~~ ). A critical component of the project is ensu... [9]

~~Deleted:~~ The first version of MIX Asian inventory ... [10]

~~Deleted:~~ MIXv1 incorporates five regional emission ... [11]

~~Deleted:~~ Li et al., 2017c). A profile-based speciation ... [12]

~~Deleted:~~ ). A profile-based speciation scheme for N... [13]

~~Deleted:~~ Li et al., 2014; Li et al., 2019b). Specificall... [14]

~~Deleted:~~ ; Li et al., 2019b). Specifically, MIXv1 adv... [15]

~~Deleted:~~ Li et al., 2019b). Specifically, MIXv1 adva... [16]

~~Deleted:~~ ). Specifically, MIXv1 advances our ... [17]

**Moved up [1]:** Tremendous efforts have been made

~~Deleted:~~ Consistent greenhouse gas emissions are cr... [18]

~~Deleted:~~ Fiore et al., 2015). Carbon dioxide (CO<sub>2</sub>) is ... [19]

~~Deleted:~~ ). Carbon dioxide (CO<sub>2</sub>) is co-emitted with ... [20]

~~Deleted:~~ Fiore et al., 2015). Previous studies have ... [21]

~~Deleted:~~ ). Previous studies have emphasized the ... [22]

~~Deleted:~~ Jacob and Winner, 2009; Saari et al., 2015) ... [23]

~~Deleted:~~ ; Saari et al., 2015), as recently summarize... [24]

~~Deleted:~~ Saari et al., 2015), as recently summarize... [25]

~~Deleted:~~ ), as recently summarized by the Synthesis ... [26]

~~Deleted:~~ Klausbrückner et al., 2016; Phillips, 2022; ... [27]

~~Deleted:~~ ; Phillips, 2022; von Schneidmesser and M... [28]

~~Deleted:~~ ; von Schneidmesser and Monks, 2013). T... [29]

~~Deleted:~~ ; von Schneidmesser and Monks, 2013). T... [30]

~~Deleted:~~ ). To address this need, CO<sub>2</sub> emissions are ... [31]

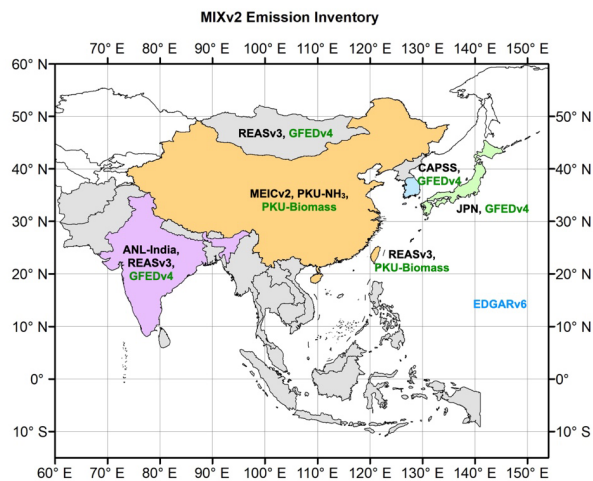
~~Deleted:~~ seven

~~Deleted:~~ the Regional Emission inventory in Asia



548 (Kurokawa and Ohara, 2020); the Multi-resolution Emission Inventory for China version 2.0  
 549 (MEICv2, <http://www.meicmodel.org>) (Li et al., 2017b; Zheng et al., 2021; Zheng et al., 2018); a  
 550 process-based NH<sub>3</sub> emission inventory developed by Peking University (referred to as PKU-NH<sub>3</sub>)  
 551 (Kang et al., 2016); an official Japan emission inventory (referred to as JPN) (Chatani et al., 2018;  
 552 Shibata and Morikawa, 2021); an Indian emission inventory for power plants from Argonne  
 553 National Laboratory (referred to as ANL-India) (Lu and Streets, 2012; Lu et al., 2011); an open  
 554 biomass burning emission inventory from Peking University (PKU-Biomass) (Yin et al., 2019);  
 555 the official emissions from Clean Air Policy Support System (CAPSS) for the Republic of Korea  
 556 (Lee et al., 2011) ; the fourth version of Global Fire Emissions Database with small fires  
 557 (GFEDv4s) (van der Werf et al., 2017); and the Emissions Database for Global Atmospheric  
 558 Research (EDGAR) version 6 for the shipping emissions (Janssens-Maenhout et al., 2019). Figure  
 559 1 shows the distribution of the components of **emission** inventories which are mosaicked into the  
 560 MIXv2.

Deleted: regional



561  
 562 **Figure 1. Components of regional emission inventories in the MIXv2 mosaic. Colors of text**  
 563 **represent the type of sources: black is anthropogenic, dark green represents open biomass**  
 564 **burning, and blue is the inland and international shipping.**

565  
 566 We follow a similar hierarchy in MIXv2 as the previous version in the mosaic process. We use  
 567 REASv3 as the default inventory for anthropogenic sources, and then further replace it with  
 568 official emission inventories at a finer scale. MEIC, PKU-NH<sub>3</sub> and ANL-India are demonstrated  
 569 as the best available inventories through inter-comparisons to represent local source distribution  
 570 with advanced methodology and reliable data sources (Li et al., 2017c). Thus, MEIC overrides  
 571 REAS for anthropogenic emissions over mainland China. PKU-NH<sub>3</sub>, which was developed with

573 a process-based model was further applied to replace the NH<sub>3</sub> emissions in MEIC. In Japan, JPN  
574 provides emissions for all air pollutants. The ratios of CO<sub>2</sub> to NO<sub>x</sub> by sectors derived from REAS  
575 are combined with JPN to develop CO<sub>2</sub> gridded emissions. In detail, we firstly calculated the  
576 total CO<sub>2</sub> emissions of Japan by multiplying the CO<sub>2</sub> to NO<sub>x</sub> ratios and JPN's NO<sub>x</sub> emission  
577 estimates by sectors, then we developed the spatial proxies based on the NO<sub>x</sub> gridded emissions  
578 of JPN. Lastly, the calculated CO<sub>2</sub> emissions were allocated to each grid month by month. We  
579 use ANL-India for SO<sub>2</sub>, NO<sub>x</sub> and CO<sub>2</sub> for power plants in India directly, and complement  
580 emissions of other species and sectors with REASv3. Regarding Hong Kong of China, we use  
581 the updated REASv3 emissions. ▽

**Deleted:** . To maintain consistency in spatial distribution, we re-located REAS power plant emissions for other species to grids based on spatial proxies derived from ANL-India.

582 The open biomass emissions of MIX are developed by combining GFEDv4s and PKU-Biomass  
583 inventories. GFED emissions over Asia are processed to the objective domain. We re-gridded the  
584 GFED emissions from 0.25 to 0.1 degree based on an area-weighted algorithm in a mass-  
585 balanced way. Wildfires of various vegetation types (including savanna, forest, peatland) and in-  
586 field agricultural waste burning are aggregated into the “open biomass burning” sector. PKU-  
587 Biomass overrides the emissions of GFED over China (including Hong Kong and Taiwan) on a  
588 both monthly and daily basis. ▽

**Deleted:**

589 The consistency of data is ensured in three aspects: source aggregation, spatial distribution, and  
590 NMVOc speciation. Firstly, a consistent source definition system was applied in source  
591 aggregation from regional emission inventories to the final emission mosaic, as outlined in Table  
592 2 and Table S1. Secondly, the consistency of emissions spatial distribution during emissions  
593 mosaic between different inventories are ensured carefully. In India, we integrated the ANL-  
594 India emissions for NO<sub>x</sub>, SO<sub>2</sub>, and CO<sub>2</sub> for pointed power plants, and emissions from REAS for  
595 other species. To keep the consistency in spatial distribution, we developed spatial proxies based  
596 on the CO<sub>2</sub> emissions from ANL-India, and re-located REAS emissions for other species.  
597 Thirdly, a consistent NMVOc speciation framework was applied throughout all component  
598 emission inventories for both anthropogenic and open biomass burning sources, which is  
599 described in detail in Sect. 2.4.

**Deleted:** ¶

605

606

**Table 1. Key features of MIXv2 and the component emission inventories.**

Items	MIXv2	REASv3.3	MEICv2.0	PKU-NH <sub>3</sub>	ANL-India	JPN	CAPSS	PKU-Biomass	GFEDv4s	EDGARv6
Anthropogenic										
Power	X	X	X	X	X	X	X			
Industry	X	X	X	X		X	X			
Residential	X	X	X	X		X	X			
Transportation	X	X	X	X		X	X			
Agriculture	X	X	X	X		X	X			
Open biomass burning	X						X	X	X	
Shipping	X									X
Temporal coverage	2010-2017	1950-2017	1990-2017	1980-2017	2010-2017	2000-2017	2000-2018	1980-2017	2010-2017	1970-2018
Temporal resolution	Monthly	Monthly	Monthly	Monthly	Monthly	Monthly	Annual	Daily	Daily	Monthly
Spatial coverage	Asia	Asia	Mainland China	Mainland China	India	Japan	Korea, Republic of	China	Global	Global
Spatial resolution (degree in horizontal)	0.1	0.1, point	0.1, point	0.1	point	0.1	0.1	0.1	0.25	0.1
Species										
NO <sub>x</sub>	X	X	X		X	X	X	X	X	X
SO <sub>2</sub>	X	X	X		X	X	X	X	X	X
CO	X	X	X			X	X	X	X	X
NM VOC	X	X	X			X	X	X	X	X

Deleted: horizontal,

NH <sub>3</sub>	X	X	X	X		X	X	X	X	X
PM <sub>10</sub>	X	X	X			X	X	X	X	X
PM <sub>2.5</sub>	X	X	X			X	X	X	X	X
BC	X	X	X			X	X	X	X	X
OC	X	X	X			X	X	X	X	X
CO <sub>2</sub>	X	X	X		X		X	X	X	X
NMVOC speciation	SAPRC99, SPARC07, CB05	19 species	SAPRC99, SPARC07, CB05	N/A	N/A	SAPRC07, CB05	N/A	N/A	26 species	N/A
Data availability	<a href="https://csl.noaa.gov/groups/csl4/modeldata/data/Li2023/">https://csl.noaa.gov/groups/csl4/modeldata/data/Li2023/</a>	<a href="https://www.nies.go.jp/REAS/index.html">https://www.nies.go.jp/REAS/index.html</a> (for REASv3.2.1) (last access: 04/2022)	<a href="http://www.meicmodel.org">www.meicmodel.org</a> (last access: 06/2022)	<a href="http://meicmodel.org.cn/?page_id=1772&amp;lang=en">http://meicmodel.org.cn/?page_id=1772&amp;lang=en</a> (last access: 06/2022)	Lu et al. (2011)	Chatani et al. (2018); Shibata and Morikawa (2021)	National Institute of Environmental Research Center	<a href="http://meicmodel.org.cn/?page_id=1772&amp;lang=en">http://meicmodel.org.cn/?page_id=1772&amp;lang=en</a> (last access: 06/2022)	<a href="https://www.globalfiredata.org/">https://www.globalfiredata.org/</a> (last access: 10/2022)	<a href="https://edgar.jrc.ec.europa.eu/">https://edgar.jrc.ec.europa.eu/</a> (last access: 10/2022)

608  
609  
610  
611  
612  
614

**Deleted:**  
 Table 3. Anthropogenic | Open biomass<sup>a</sup> emissions of MIXv2 by Asian countries and regions in 2017. Country ... [33]

620

**Table 2. Sector and subsectors included in MIXv2<sup>a</sup>.**

Sector	Subsector	IPCC code <sup>b</sup>
Power	Power plants	1A1a
Industry	Industrial coal combustion	1A2, 1A1c
	Industrial other fuel combustion	1A2
	Chemical industry	1B2b, 2B
	Oil production, distribution, and refinery	1B2a
	Other industrial process	2A1, 2A2, 2A7, 2C, 2
	Industrial paint use	3A
	Solvent use other than paint	3B, 3C
Residential	Residential coal combustion	1A4b
	Residential biofuel combustion	1A4bx
	Residential other fuel combustion	1A4b
	Waste treatment	6A, 6C
	Domestic solvent use	3C
Transportation	On-road gasoline	1A3b
	On-road diesel	1A3b
	Off-road diesel	1A3c, 1A4c
Agriculture	Livestock	4B
	Fertilizer use	4D
Open biomass burning	Agriculture in-field burning	4F
	Fires	4E, 5A, 5C, 5D
Shipping	Domestic shipping	1A3d
	International shipping	1C2

621 <sup>a</sup> Detailed source profiles assigned to sources within each subsector are summarized in Table S1.622 <sup>b</sup> Reference report: [https://www.ipcc.ch/report/ar6/wg3/downloads/report/IPCC\\_AR6\\_WGIII\\_FOD\\_AnnexII.pdf](https://www.ipcc.ch/report/ar6/wg3/downloads/report/IPCC_AR6_WGIII_FOD_AnnexII.pdf)

623

624 **2.3 Components of regional emission inventory**625 **REASv3 for Asia.**

626 We used anthropogenic emissions from REASv3.3 developed by ACAP (Asia Center for Air  
627 Pollution Research) and NIES (National Institute for Environmental Studies) to fill the gaps  
628 where local inventories are not available. REASv3 was developed as a long historical emission  
629 inventory for Asia from 1950 - 2015 with monthly variations and relatively high spatial  
630 resolution (0.25 degree). Compared to previous versions, REASv3 updated the emission factors  
631 and information on control policies to reflect the effect of emission control measures, especially

632 for East Asia. Large power plants are treated as point sources and assigned with coordinates of  
633 locations. In REASv3, power plants constructed after 2008 with generation capacity larger than  
634 300 MW are added as point sources. Additionally, REASv3 updated the spatial and temporal  
635 allocation factors for the areal sources. Emissions of Japan, the Republic of Korea and Taiwan  
636 are originally estimated in the system. The REASv3 data were further developed to 2017  
637 following the same methodology as Kurokawa et al. (2020) and updated to a finer spatial  
638 resolution of 0.1 degree except for NH<sub>3</sub> emissions from fertilizer application where grid  
639 allocation factor for 0.1 degree were prepared from that of 0.25 degree for REASv3.2.1 assuming  
640 homogeneous distribution of emissions in each 0.25-degree grid cell. We used the REAS  
641 estimates for Taiwan directly and replaced REAS with local inventories as illustrated below.

642

#### 643 **MEICv2 for China.**

644 For China, we used the anthropogenic emissions from the MEIC model developed and  
645 maintained by Tsinghua University. MEIC uses a technology-based methodology to quantify air  
646 pollutants and CO<sub>2</sub> from more than 700 emitting sources since 1990 (Li et al., 2017b).  
647 Specifically, MEIC has developed a unit-based power plant database, a comprehensive vehicle  
648 modeling approach and a profile-based NMVOC speciation framework. Detailed methodology  
649 and data sources can be found in previous MEIC studies (Li et al., 2017b; Liu et al., 2015; Zheng  
650 et al., 2014). In version 2.0, iron and steel plants, and cement factories are also treated as point  
651 sources, which is important to improve industrial emissions estimation (Zheng et al., 2021).  
652 MEIC is an online data platform publicly available to the community for emissions calculation,  
653 data processing and data downloading. MEIC delivers monthly emissions at various spatial  
654 resolutions and chemical mechanisms as defined by the user. We downloaded the emissions at  
655 0.1 degree generated from MEIC v2.0 and aggregated it to five anthropogenic sectors: power,  
656 industry, residential, transportation and agriculture. We followed the speciation framework in the  
657 MEIC model and applied it to other regions of Asia, as described in detail in Sect. 2.4. MEIC  
658 emissions of SAPRC99, SAPRC07 and CB05 were used directly in MIX.

659

#### 660 **PKU-NH<sub>3</sub> for NH<sub>3</sub>, China.**

661 We replaced MEIC with the high-resolution PKU-NH<sub>3</sub> inventory for NH<sub>3</sub> emissions in China  
662 developed by Peking University (Huang et al., 2012b; Kang et al., 2016). PKU-NH<sub>3</sub> uses a  
663 process-based model to compile NH<sub>3</sub> emissions with emission factors that vary with ambient  
664 temperature, soil property, and the method and rate of fertilizer application (Huang et al., 2012b).  
665 Compared to the previous version used in MIXv1, PKU-NH<sub>3</sub> further refined emission factors by  
666 adding the effects of wind speed and in-field experimental data of NH<sub>3</sub> flux in northern China  
667 cropland. Emissions are allocated to 1km × 1km grids using spatial proxies derived from a land  
668 cover dataset, rural population, etc (Huang et al., 2012b). Monthly emissions over China,  
669 including Hong Kong, Macao, and Taiwan are available from 1980 to 2017. We aggregated the 9  
670 sub-sectors into 5 MIX anthropogenic sectors (power, industry, residential, transportation,  
671 agriculture) and excluded the agricultural in-field waste burning.

672

673 **ANL-India for power plants, India.**

674 ANL-India is a continuously-updated long-term power plant emission inventory for India  
675 developed on a unit and monthly basis by Argonne National Laboratory (Lu and Streets, 2012;  
676 Lu et al., 2011). Emissions are calculated for more than 1300 units in over 300 thermal power  
677 plants based on the detailed information collected from various reports of the Central Electricity  
678 Authority (CEA) in India. As much as possible, the accurate and actual operational data of power  
679 units/plants are used in inventory development, including geographical locations, capacity,  
680 commissioning and retirement time, actual monthly power generation, emission control  
681 application, fuel type, source, specifications, and consumption, etc. Detailed method can be  
682 found in Lu et al. (2011) and Lu and Streets (2012). ANL-India is available for NO<sub>x</sub>, SO<sub>2</sub> and  
683 CO<sub>2</sub>. In this work, the 2010-2017 period of ANL-India at the monthly level is used directly in  
684 MIX. We further merged ANL-India with REASv3 for other species to complete the emission  
685 estimation in India. CO<sub>2</sub> emissions of ANL-India at 0.1°× 0.1° grids were used to develop spatial  
686 proxies by sectors, year, and month. Then, REASv3 emissions of all other species were re-  
687 allocated to grids based on ANL derived spatial proxies. Although ANL-India provides  
688 emissions by fuel type, the fuel heterogeneity of thermal power plants is not considered in the re-  
689 gridding process of MIX here because about 93% of the thermal power generation in India  
690 during 2010-2017 were fueled with coal (Lu and Streets, 2012).

691

692 **JPN (PM2.5EI and J-STREAM) for Japan.**

693 We used the JPN inventory to override the Japan emissions of REAS. JPN was jointly developed  
694 by the Ministry of Environment, Japan (MOE-J) for mobile source emissions (i.e., PM2.5 EI)  
695 and by the National Institute of Environmental Studies (NIES) for stationary source emissions (J-  
696 STREAM). Major anthropogenic sources are included in PM2.5EI, with vehicle emissions  
697 explicitly estimated in detail (Shibata and Morikawa, 2021). Emission factors are assigned as a  
698 function of average vehicle velocity by 13 vehicle types and regulation years. The hourly  
699 average vehicle type of trunk roads and narrow roads are obtained from in-situ measurements. In  
700 addition to the running emission exhaust, emissions from engine starting, evaporation, tire wear,  
701 road dust and off-road engines are also estimated. To keep consistency with the sector definition  
702 of MIX, we excluded the road dust aerosol emissions and mapped other sources to five  
703 anthropogenic sectors. For stationary sources, Japan emissions are derived from the Japan's  
704 Study for Reference Air Quality Modeling (J-STREAM) model intercomparison project (Chatani  
705 et al., 2020; Chatani et al., 2018). Long-term emissions of over 100,000 large stationary sources  
706 are estimated based on energy consumption and emission factors derived from the emission  
707 reports submitted to the government every three years (Chatani et al., 2020). NMVOC emissions  
708 are speciated into SAPRC07 and CB05 using local source profiles. Emissions are distributed to  
709 1km × 1km grids with monthly variations based on spatial and temporal proxies. We re-sampled  
710 the monthly JPN emissions to 0.1°× 0.1° grids and merged them into MIXv2.

711



712 **CAPSS for the Republic of Korea.**

713 For the Republic of Korea, we use the official emissions from CAPSS developed by the National  
714 Institute of Environmental Research Center (Lee et al., 2011). CAPSS estimated the annual  
715 emissions of air pollutants of CO, NO<sub>x</sub>, SO<sub>x</sub>, PM<sub>10</sub>, PM<sub>2.5</sub>, BC, NMVOCs and NH<sub>3</sub> based on the  
716 statistical data collected from 150 domestic institutions since 1990s (Crippa et al., 2023). There  
717 are inconsistencies on the long-term emissions trend of CAPSS due to data and methodology  
718 changes over the time. We used the re-analyzed data of CAPSS during 2010-2017, which  
719 updated the emission factors and added the missing sources. Point sources, area sources, and  
720 mobile sources were processed using source-based spatial allocation methods (Lee et al., 2011).  
721 Monthly variations by sectors are derived from REASv3 for the Republic of Korea and were  
722 further applied to CAPSS. In MIXv2, the monthly gridded emissions allocated at 0.1-degree  
723 grids for the anthropogenic sector (power, industry, residential, transportation, agriculture) of  
724 CAPSS are integrated.

725

726 **GFEDv4s for open biomass burning, Asia.**

727 Emissions over Asia from GFEDv4s database with small fires were used as the default inventory  
728 for open biomass burning sources. GFED quantified global fire emissions patterns based on the  
729 Carnegie-Ames-Stanford Approach (CASA) biogeochemical model from 1997 onwards (van der  
730 Werf et al., 2017). Compared to previous versions, higher quality input datasets from different  
731 satellite and in situ data streams are used, and better parameterizations of fuel consumption and  
732 burning processes are developed. We calculated emissions for trace gases, aerosol species and  
733 CO<sub>2</sub> based on the burned biomass and updated emission factors by vegetation types provided by  
734 the GFED dataset (Akagi et al., 2011; Andreae and Merlet, 2001). Monthly and daily emissions  
735 were re-gridded from 0.25° to 0.1° and cropped to a unified domain as anthropogenic emissions.  
736 Open fires of grassland, shrubland, savanna, forest, and agricultural waste burning are included.  
737 We assigned profiles for each source category as listed in Table S1. Model-ready emissions of  
738 SAPRC99, SAPRC07 and CB05 were lumped from individual species as described in Sect. 2.4.  
739 GFED emissions are further replaced by PKU-Biomass over China.

740

741 **PKU-Biomass for biomass burning, China.**

742 China's emissions estimated by the PKU-Biomass inventory were used to override GFED  
743 emissions for open biomass burning in MIXv2. PKU-Biomass is developed by Peking University  
744 based on the MODIS fire radiative energy data for China from 1980 to 2017 (Huang et al.,  
745 2012a; Song et al., 2009; Yin et al., 2019). Emission factors of both air pollutants and CO<sub>2</sub> are  
746 assigned for four types of biomass burning types including forest, grassland, shrubland fires and  
747 agricultural waste burning. PKU-Biomass takes account of the farming system and crop types in  
748 different temperate zones. High-resolution emissions (1km) with daily variations are available.  
749 We re-gridded emissions to 0.1° × 0.1° and aggregated the emissions to the “open biomass  
750 burning” sector. An explicit source profile assignment approach was assigned to each vegetation

751 type. Emissions of three chemical mechanisms were further developed for PKU-Biomass and  
752 merged into the MIXv2 final dataset over Asia.

753

#### 754 **EDGARv6 for shipping, Asia.**

755 We used the shipping (domestic and international) emissions over Asia derived from EDGARv6  
756 in MIXv2. EDGAR is a globally consistent emission inventory for anthropogenic sources  
757 developed by the Joint Research Centre of the European Commission (Crippa et al., 2018;  
758 Janssens-Maenhout et al., 2019). Emissions of both air pollutants and greenhouse gases are  
759 estimated. EDGAR uses international statistics as activity data and emission factors varying with  
760 pollutants, sector, technology, and abatement measures for emissions calculation for 1970-2018.  
761 Shipping route data are used as spatial proxies to distribute emission estimates to 0.1-degree  
762 grids. We downloaded the emissions data for both inland and international shipping from 2010 to  
763 2017, processed the data to the MIX domain and aggregated them to the “Shipping” sector.  
764 Monthly emissions are only available for 2018. We applied the monthly variations of air  
765 pollutants in 2018 to emissions of 2010-2017 accordingly.

766

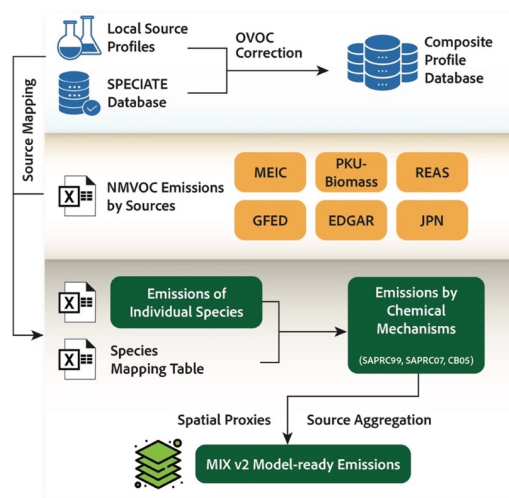
#### 767 **2.4 NMVOC speciation**

768 NMVOC speciation has substantial impacts on the model-ready emissions accuracy and  
769 performance of chemical transport models (Li et al., 2014). Selection of profiles turns out to be  
770 the most important contributor to uncertainties in emissions of individual species. To reduce the  
771 uncertainties due to the inaccurate species mapping, Li et al. (2014) developed an explicit  
772 assignment approach based on multiple profiles and mechanism-dependent mapping tables.

773 We processed the gas-phase speciation for NMVOCs following the profile-based mapping  
774 procedure, as shown in Fig. 2. The speciation was conducted at a detailed source basis. Firstly,  
775 we developed the composite source profile database by combining the US EPA’s SPECIATE  
776 database v4.5 (last access: June 2019) (Simon et al., 2010) and available local measurements  
777 (e.g., Akagi et al., 2011; Mo et al., 2016; Xiao et al., 2018; Yuan et al., 2010). The complete list  
778 of source profiles used in this work is provided in Table S1. To diminish the uncertainties due to  
779 inappropriate sampling and analyses techniques regarding Oxygenated Volatile Organic  
780 Compounds (OVOCs), we applied the OVOC correction to those incomplete profiles. The  
781 detailed method can be found in previous studies (Li et al., 2014). Especially, the following  
782 sources have significant OVOC emitted which should be addressed: coal combustion in  
783 residential stoves (31%), residential wood and crop residue fuel use (23% ~ 33%) and diesel  
784 engines (28% ~ 47%). Secondly, we assigned the composite profile database to each component  
785 inventory to develop emissions of individual species. Lastly, individual species were lumped to  
786 three chemical mechanisms (SAPRC99, SAPRC07, CB05) based on the conversion factors  
787 derived from mechanism-dependent mapping tables (Carter, 2015).

788 For the Republic of Korea and Hong Kong, we applied the speciation factor for SAPRC99 and  
789 CB05 by sectors developed from the SMOKE-Asia model, which have been used for MIXv1

790 (Woo et al., 2012). Emissions of SAPRC07 were further developed from SAPRC99 based on  
 791 Table S2, which applied MEIC speciated results.



792 **Figure 2. NMVOC speciation scheme used in MIXv2.**

793  
 794  
 795 **2.5 Limitations and Uncertainties**

796 As a mosaic inventory, MIXv2 has several limitations when integrating various gridded products  
 797 into a unified dataset. Firstly, inconsistencies could exist at country boundaries where different  
 798 datasets were used for the adjacent countries (Janssens-Maenhout et al., 2015), for example, the  
 799 border between China and India. But limited effects are anticipated here given the small area  
 800 affected due to the high spatial resolution and the low population density at the border. Secondly,  
 801 extracting emissions by country from gridded maps may introduce uncertainties especially for  
 802 power plants located near the coast. This issue is more important because gridded emissions are  
 803 developed with higher spatial resolutions than earlier versions. Using an extended country map  
 804 by assigning extra adjacent grids of “ocean” with the neighboring country can reduce this bias.  
 805 We also acknowledge the general inconsistency of uncertainty levels between countries where  
 806 different inventories are used following various data sources and approaches. For air quality  
 807 simulation purposes, the lack of diurnal variations and vertical distribution is another limitation  
 808 when applying MIXv2 data directly. Development of Asia-specific temporal and vertical profiles  
 809 is important to improve the model simulation performance in the future.

Deleted:

810 It's always difficult to quantify the uncertainties for a mosaic emission inventory such as MIXv2.  
 811 The uncertainties for each of the component inventories are discussed in detail in corresponding

813 studies (Kang et al., 2016; Kurokawa and Ohara, 2020; Yin et al., 2019; Zheng et al., 2018).  
814 Here we summarized the uncertainty estimation by Asian regions in previous studies in Table 3.  
815 The uncertainty ranges are quantified based on propagation of uncertainty (Kurokawa and Ohara,  
816 2020; Lei et al., 2011; Zhang et al., 2009) or thousands of Monte Carlo simulations (Lu et al.,  
817 2011; Paliwal et al., 2016; Shan et al., 2020; Shi and Yamaguchi, 2014; Sun et al., 2018; Zhao et  
818 al., 2011; Zhao et al., 2012; Zhao et al., 2013; Zhou et al., 2017).

819 In regard of anthropogenic sectors, the precision of emission estimates for SO<sub>2</sub>, NO<sub>x</sub>, and CO<sub>2</sub> is  
820 higher than that of other pollutants, owing to the minimal uncertainties associated with power  
821 plants and large industrial facilities. This is particularly notable in the case of MIXv2, where  
822 uncertainties are even lower due to the integration of unit-based power plant information for both  
823 China and India. While uncertainties for CO and NMVOC are comparable, they are higher than  
824 those for SO<sub>2</sub>, NO<sub>x</sub>, and CO<sub>2</sub>, because of substantial emission contributions from biofuel  
825 combustion. Emissions for particulate matter (especially BC and OC) tend to be more uncertain  
826 compared to trace gases, primarily due to the low data availability of accurate activity rates and  
827 emission factors related to residential biofuel combustion. The need for more detailed  
828 information at the technology or facility level in regions, such as India, OSA, and SEA, is crucial  
829 to narrow down the overall uncertainties in Asia in the future. For open biomass burning,  
830 previous investigations have estimated low uncertainty ranges for species like CO, NMVOC, and  
831 OC, while more further analyses are in urgent need. In this work, we conducted uncertainty  
832 analyses qualitatively by comparing the MIXv2 estimates with other bottom-up inventories and  
833 those derived from satellite retrievals in Sect. 4 (Li et al., 2018). In short summary, generally  
834 consistent emission estimates and trends over Asia are found based on bottom-up and top-down  
835 comparisons in Sect. 4. Discrepancies persist, especially in regions like South Asia and Southeast  
836 Asia, as well as among species like BC and NMVOC.

Deleted: Here w

**Table 3. Uncertainties in emission estimates by Asian regions (95% confidence intervals if not noted; unit: %).**

Deleted: 1

Regions, Anthropogenic or Open Biomass	NO <sub>x</sub>	SO <sub>2</sub>	NO <sub>x</sub>	CO	NMVOG	NH <sub>3</sub>	PM <sub>10</sub>	PM <sub>2.5</sub>	BC	OC	CO <sub>2</sub>	Year	Reference
China, Anthropogenic							±91	±107	±187	±229		2005	Lei et al. (2011)
	-13~37	-14~13	-13~37				-14~45	-17~54	-25~136	-40~121		2005	Zhao et al. (2011)
				-20~45								2005	Zhao et al. (2012)
	±31	±12	±31	±70	±68		±132	±130	±208	±258		2006	Zhang et al. (2009)
		-16~17							-41~80	-44~92		2010	Lu et al. (2011)
	-15~35	-15~26	-15~35	-18~42			-15~54	-15~63	-28~126	-42~114		2010	Zhao et al. (2013)
	±35	±40	±35	±73	±76	±82	±83	±94	±111	±193	±19	2015	Kurokawa et al. (2020)
	-26~34	-22~25	-26~34	-31~41	-32~56							2015	Sun et al. (2018)
						-14~13					2015	Zhang et al. (2017)	
										-15~30	2017	Shan et al. (2020)*	
India, Anthropogenic		-15~16							-41~87	-44~92		2010	Lu et al. (2011)
	±35	±41	±35	±136	±115	±111	±120	±151	±133	±233	±27	2015	Kurokawa et al. (2020)
									±33			2011	Paliwal et al. (2016)
Japan, Anthropogenic	±32	±34	±32	±45	±63	±103	±68	±74	±58	±100	±13	2015	Kurokawa et al. (2020)
OEA, Anthropogenic	±60	±38	±60	±67	±63	±94	±69	±85	±82	±168	±19	2015	Kurokawa et al. (2020)
OSA, Anthropogenic	±34	±40	±34	±87	±73	±93	±96	±112	±124	±211	±19	2015	Kurokawa et al. (2020)
SEA, Anthropogenic	±38	±46	±38	±124	±86	±115	±125	±155	±161	±232	±25	2015	Kurokawa et al. (2020)
China, Biomass	-37~37	-54~54	-37~37	-4~4	-9~9	-49~48	-7~6	-13~1	-61~61	-20~19	-3~3	2012	Zhou et al. (2017)
SEA, Biomass	±23	±30	±23	±20	±18	±10			±20	±31	±15	2010	Shi and Yamaguchi (2014)

\* 97% Confidence Interval

**Table 4. Anthropogenic | Open biomass<sup>a</sup> emissions of MIXv2 by Asian countries and regions in 2017.**

<u>Country</u>	<u>NO<sub>x</sub><sup>b</sup></u>	<u>SO<sub>2</sub></u>	<u>CO</u>	<u>NMVOC</u>	<u>NH<sub>3</sub></u>	<u>PM<sub>10</sub></u>	<u>PM<sub>2.5</sub></u>	<u>BC</u>	<u>OC</u>	<u>CO<sub>2</sub><sup>b</sup></u>
<b><u>China<sup>c</sup></u></b>	<b><u>22.37   0.22</u></b>	<b><u>10.62   0.02</u></b>	<b><u>137.02   4.40</u></b>	<b><u>29.36   1.66</u></b>	<b><u>9.18   0.08</u></b>	<b><u>10.20   0.41</u></b>	<b><u>7.65   0.35</u></b>	<b><u>1.26   0.03</u></b>	<b><u>2.09   0.17</u></b>	<b><u>11.34   0.07</u></b>
<u>Japan</u>	<u>1127.0   8.4</u>	<u>274.8   1.5</u>	<u>2543.1   192.0</u>	<u>927.1   141.2</u>	<u>397.7   2.9</u>	<u>84.3   30.1</u>	<u>40.7   19.6</u>	<u>14.9   1.3</u>	<u>7.5   11.9</u>	<u>785.9   3.4</u>
<u>Korea, DPR</u>	<u>194.6   3.5</u>	<u>83.8   0.7</u>	<u>2580.5   92.7</u>	<u>140.4   61.7</u>	<u>107.4   1.6</u>	<u>96.6   13.5</u>	<u>52.6   9.3</u>	<u>10.0   0.6</u>	<u>16.4   5.4</u>	<u>29.7   1.5</u>
<u>Korea, Republic of</u>	<u>979.1   2.8</u>	<u>266.7   0.5</u>	<u>522.1   61.0</u>	<u>917.1   44.5</u>	<u>292.5   0.9</u>	<u>127.6   9.5</u>	<u>64.5   6.2</u>	<u>11.2   0.4</u>	<u>31.3   3.7</u>	<u>581.9   1.1</u>
<u>Mongolia</u>	<u>125.5   28.3</u>	<u>124.9   7.8</u>	<u>1057.9   945.5</u>	<u>50.3   368.7</u>	<u>196.1   17.6</u>	<u>45.5   129.7</u>	<u>20.6   110.3</u>	<u>2.7   4.2</u>	<u>3.5   62.7</u>	<u>18.3   14.2</u>
<b><u>Other East Asia<sup>c,d</sup></u></b>	<b><u>2.43   0.04</u></b>	<b><u>0.75   0.01</u></b>	<b><u>6.70   1.29</u></b>	<b><u>2.03   0.62</u></b>	<b><u>0.99   0.02</u></b>	<b><u>0.35   0.18</u></b>	<b><u>0.18   0.15</u></b>	<b><u>0.04   0.01</u></b>	<b><u>0.06   0.08</u></b>	<b><u>1.42   0.02</u></b>
<b><u>India<sup>c</sup></u></b>	<b><u>9.34   0.11</u></b>	<b><u>13.82   0.01</u></b>	<b><u>61.23   1.91</u></b>	<b><u>14.46   1.23</u></b>	<b><u>9.87   0.03</u></b>	<b><u>7.20   0.27</u></b>	<b><u>4.97   0.18</u></b>	<b><u>0.86   0.01</u></b>	<b><u>1.72   0.09</u></b>	<b><u>2.88   0.04</u></b>
<u>Afghanistan</u>	<u>83.2   0.2</u>	<u>45.0   0.0</u>	<u>560.2   2.7</u>	<u>131.2   1.4</u>	<u>320.3   0.0</u>	<u>39.9   0.4</u>	<u>30.7   0.3</u>	<u>8.3   0.0</u>	<u>12.1   0.1</u>	<u>11.1   0.1</u>
<u>Bangladesh</u>	<u>342.3   2.8</u>	<u>224.5   0.3</u>	<u>3074.5   41.9</u>	<u>836.0   15.7</u>	<u>922.5   0.5</u>	<u>685.6   5.8</u>	<u>350.1   4.4</u>	<u>43.6   0.2</u>	<u>114.3   2.0</u>	<u>127.7   0.9</u>
<u>Bhutan</u>	<u>0.8   1.0</u>	<u>0.5   0.4</u>	<u>31.5   30.0</u>	<u>6.4   14.8</u>	<u>2.8   0.3</u>	<u>13.6   5.9</u>	<u>5.1   4.3</u>	<u>0.4   0.2</u>	<u>1.2   3.1</u>	<u>0.8   0.6</u>
<u>Maldives</u>	<u>0.6   0.0</u>	<u>0.3   0.0</u>	<u>1.3   0.0</u>	<u>0.5   0.0</u>	<u>0.0   0.0</u>	<u>0.0   0.0</u>	<u>0.0   0.0</u>	<u>0.0   0.0</u>	<u>0.0   0.0</u>	<u>0.1   0.0</u>
<u>Nepal</u>	<u>70.6   7.0</u>	<u>61.2   2.2</u>	<u>2143.1   189.7</u>	<u>483.5   94.9</u>	<u>263.8   1.9</u>	<u>238.0   36.5</u>	<u>159.6   26.5</u>	<u>24.3   1.1</u>	<u>79.1   19.1</u>	<u>42.8   3.6</u>
<u>Pakistan</u>	<u>638.7   6.7</u>	<u>1607.7   0.6</u>	<u>9000.4   133.3</u>	<u>2134.7   126.9</u>	<u>1890.5   2.7</u>	<u>1479.4   16.5</u>	<u>914.0   8.9</u>	<u>108.6   1.0</u>	<u>327.6   3.3</u>	<u>308.8   2.2</u>
<u>Sri Lanka</u>	<u>205.0   2.2</u>	<u>84.7   0.2</u>	<u>1356.4   31.2</u>	<u>390.7   21.3</u>	<u>99.6   0.5</u>	<u>144.5   4.0</u>	<u>101.0   2.8</u>	<u>19.0   0.2</u>	<u>46.8   1.0</u>	<u>39.5   0.7</u>
<b><u>Other South Asia<sup>c,e</sup></u></b>	<b><u>1.34   0.02</u></b>	<b><u>2.02   0.00</u></b>	<b><u>16.17   0.43</u></b>	<b><u>3.98   0.27</u></b>	<b><u>3.50   0.01</u></b>	<b><u>2.60   0.07</u></b>	<b><u>1.56   0.05</u></b>	<b><u>0.20   0.00</u></b>	<b><u>0.58   0.03</u></b>	<b><u>0.53   0.01</u></b>
<u>Brunei</u>	<u>9.4   0.1</u>	<u>2.7   0.0</u>	<u>24.8   1.9</u>	<u>26.5   0.4</u>	<u>1.4   0.0</u>	<u>4.6   0.2</u>	<u>1.7   0.1</u>	<u>0.1   0.0</u>	<u>0.1   0.1</u>	<u>4.3   0.0</u>
<u>Cambodia</u>	<u>74.2   189.7</u>	<u>78.7   16.7</u>	<u>1155.5   2899.1</u>	<u>230.1   943.7</u>	<u>85.2   34.2</u>	<u>170.0   397.9</u>	<u>87.9   301.7</u>	<u>9.8   16.7</u>	<u>33.3   133.5</u>	<u>26.3   62.7</u>
<u>Indonesia</u>	<u>2560.0   86.3</u>	<u>3260.5   9.2</u>	<u>16039.6   2439.6</u>	<u>5438.5   559.2</u>	<u>1848.0   26.4</u>	<u>1258.0   264.6</u>	<u>839.1   188.3</u>	<u>136.5   8.9</u>	<u>338.5   97.1</u>	<u>619.0   36.6</u>
<u>Laos</u>	<u>61.4   115.8</u>	<u>126.2   10.0</u>	<u>296.3   1641.4</u>	<u>55.5   569.9</u>	<u>69.5   18.4</u>	<u>93.7   224.4</u>	<u>39.7   173.2</u>	<u>3.2   9.5</u>	<u>9.2   74.0</u>	<u>20.0   36.9</u>

Malaysia	627.1   8.6	250.3   0.8	1234.6   167.2	1029.2   65.9	237.2   2.1	226.7   20.5	137.0   14.5	14.4   0.9	13.7   6.6	224.7   3.0
Myanmar	185.5   233.3	315.9   23.4	3168.3   3576.8	936.1   1280.0	679.1   40.6	292.3   510.1	206.2   387.9	32.3   20.7	104.2   182.8	68.3   78.0
Philippines	881.4   10.1	974.2   0.8	3705.7   139.1	1031.0   91.8	469.9   1.9	315.8   18.0	197.5   12.7	39.7   0.9	61.4   4.7	159.0   3.0
Singapore	78.0   0.0	74.8   0.0	55.4   0.1	286.8   0.1	4.4   0.0	77.0   0.0	60.8   0.0	0.9   0.0	0.3   0.0	44.7   0.0
Thailand	1081.5   72.7	337.3   6.1	5073.4   1056.3	1546.1   585.4	631.0   14.3	522.8   139.3	367.1   99.7	45.5   6.6	119.5   39.9	328.2   22.6
Vietnam	546.8   44.1	517.0   3.7	6224.7   664.2	1335.1   364.1	734.0   9.2	671.9   87.7	390.1   62.2	54.3   4.2	143.0   25.3	274.5   13.9
<b>Southeast Asia<sup>c</sup></b>	<b>6.11   0.76</b>	<b>5.94   0.07</b>	<b>36.98   12.59</b>	<b>11.91   4.46</b>	<b>4.76   0.15</b>	<b>3.63   1.66</b>	<b>2.33   1.24</b>	<b>0.34   0.07</b>	<b>0.82   0.56</b>	<b>1.77   0.26</b>
<b>Asia (2017)<sup>c</sup></b>	<b>41.61   1.15</b>	<b>33.16   0.12</b>	<b>258.22   20.61</b>	<b>61.79   8.24</b>	<b>28.32   0.29</b>	<b>24.00   2.59</b>	<b>16.69   1.97</b>	<b>2.71   0.12</b>	<b>5.28   0.93</b>	<b>17.95   0.40</b>
Asia 2010/2017 <sup>f</sup>	<b>1.04   1.56</b>	<b>1.32   1.55</b>	<b>1.20   1.49</b>	<b>0.89   1.36</b>	<b>0.96   1.39</b>	<b>1.21   1.61</b>	<b>1.23   1.61</b>	<b>1.17   1.52</b>	<b>1.25   1.64</b>	<b>0.86   1.58</b>
Asia 2011/2017	<b>1.10   1.33</b>	<b>1.39   1.45</b>	<b>1.18   1.88</b>	<b>0.92   1.29</b>	<b>0.96   1.52</b>	<b>1.23   1.64</b>	<b>1.25   1.60</b>	<b>1.19   1.30</b>	<b>1.26   1.74</b>	<b>0.93   1.55</b>
Asia 2012/2017	<b>1.12   1.65</b>	<b>1.39   1.86</b>	<b>1.17   2.22</b>	<b>0.95   1.62</b>	<b>0.98   1.87</b>	<b>1.23   2.02</b>	<b>1.24   1.98</b>	<b>1.19   1.62</b>	<b>1.25   2.16</b>	<b>0.96   1.88</b>
Asia 2013/2017	<b>1.09   1.49</b>	<b>1.32   1.59</b>	<b>1.15   1.89</b>	<b>0.96   1.42</b>	<b>1.00   1.65</b>	<b>1.19   1.78</b>	<b>1.21   1.74</b>	<b>1.17   1.53</b>	<b>1.21   1.87</b>	<b>0.96   1.67</b>
Asia 2014/2017	<b>1.04   2.51</b>	<b>1.21   2.85</b>	<b>1.10   4.18</b>	<b>0.98   2.39</b>	<b>1.00   3.17</b>	<b>1.13   3.44</b>	<b>1.14   3.31</b>	<b>1.11   2.45</b>	<b>1.16   3.72</b>	<b>0.97   3.15</b>
Asia 2015/2017	<b>1.01   3.05</b>	<b>1.12   3.72</b>	<b>1.06   6.36</b>	<b>0.97   3.08</b>	<b>1.01   4.46</b>	<b>1.05   4.73</b>	<b>1.07   4.49</b>	<b>1.05   2.85</b>	<b>1.09   5.22</b>	<b>0.97   4.25</b>
Asia 2016/2017	<b>0.99   1.28</b>	<b>1.05   1.28</b>	<b>1.01   1.32</b>	<b>0.98   1.27</b>	<b>1.01   1.25</b>	<b>1.00   1.36</b>	<b>1.01   1.32</b>	<b>1.01   1.27</b>	<b>1.04   1.35</b>	<b>0.97   1.31</b>

844

845 <sup>a</sup> Anthropogenic includes power, industry, residential, transportation and agriculture. Open biomass represents the “Open Biomass Burning” sector.

846 <sup>b</sup> Tg yr<sup>-1</sup> for CO<sub>2</sub>, Gg yr<sup>-1</sup> for other species.

847 <sup>c</sup> Bold values are with the following units: Pg yr<sup>-1</sup> for CO<sub>2</sub>, Tg yr<sup>-1</sup> for other species.

848 <sup>d</sup> Other East Asia represents East Asia other than China.

849 <sup>e</sup> Other South Asia represents South Asia other than India.

850 <sup>f</sup> Asia (year/2017) represents the ratio of emissions (year) to emissions (2017) for all of Asia within the MIXv2 domain.



851

## 852 3. Results and Discussions

### 853 3.1 Asian emissions in 2017

854 In 2017, MIXv2 estimated emissions of Asia as follows: 41.6 Tg NO<sub>x</sub>, 33.2 Tg SO<sub>2</sub>, 258.2 Tg  
855 CO, 61.8 Tg NMVOC, 28.3 Tg NH<sub>3</sub>, 24.0 Tg PM<sub>10</sub>, 16.7 Tg PM<sub>2.5</sub>, 2.7 Tg BC, 5.3 Tg OC, and  
856 18.0 Pg CO<sub>2</sub> for all anthropogenic sources including power, industry, residential, transportation  
857 and agriculture. Emissions are summarized by Asian regions, including China, East Asia Other  
858 than China (OEA), India, South Asia other than India (OSA) and Southeast Asia (SEA), as  
859 shown in Table 4. China, India, and SEA together account for > 90% of the total Asian  
860 emissions. China dominates the emissions (> 50%) of CO<sub>2</sub> (11.3 Pg, 63%), NO<sub>x</sub> (22.4 Tg, 54%),  
861 and CO (137.0 Tg, 53%), and contributes more than 30% to all other species. The contributions  
862 of India are larger than 30% for SO<sub>2</sub> (13.8 Tg, 42%), NH<sub>3</sub> (9.8 Tg, 35%), BC (0.86 Tg, 32%),  
863 OC (1.7 Tg, 33%), PM<sub>10</sub> (7.2 Tg, 30%), and PM<sub>2.5</sub> (5.0 Tg, 30%). SEA ranks 3<sup>rd</sup> for all species,  
864 including CO<sub>2</sub> (1.8 Pg, 10%), NO<sub>x</sub> (6.1 Tg, 15%), SO<sub>2</sub> (5.9 Tg, 18%), NMVOC (11.9 Tg, 19%),  
865 NH<sub>3</sub> (4.8 Tg, 17%), and ~15% of aerosol species. OEA's share varies from 1% (aerosol species)  
866 to 8% (CO<sub>2</sub>). Emission proportions of OSA are around 11% for NH<sub>3</sub>, OC, and PM<sub>10</sub>, and less  
867 than 10% for others.

868 Sectoral contribution varies among species in Asia, according to our estimates. Power plants  
869 contribute significantly to SO<sub>2</sub> (1<sup>st</sup> contributor, 38%) and CO<sub>2</sub> (2<sup>nd</sup> contributor, 33%). Industry  
870 dominates the emissions of CO<sub>2</sub> (41%), NMVOC (44%), PM<sub>2.5</sub> (39%), and PM<sub>10</sub> (47%). For  
871 NO<sub>x</sub>, transportation accounts for 33% of the total emissions, followed by industry (24%) and  
872 inland and international shipping (18%). The residential sector contributes > 38% of emissions  
873 for PM<sub>2.5</sub>, BC, CO, and OC. NH<sub>3</sub> is dominated by agriculture (81%), followed by 13% from  
874 residential.

875 Open biomass burning plays a key role in SEA and OEA's emissions budget, and is a minor  
876 contributor for other regions, as shown in Table 4 and Figure 3. Including the open biomass  
877 burning sector increases the emissions of OC, PM<sub>2.5</sub>, PM<sub>10</sub>, NMVOC, CO and CO<sub>2</sub>, by 69%,  
878 53%, 46%, 37%, 34% and 15%, respectively for SEA. Due to the active fire events, Southeast  
879 Asia is the largest emission contributor for OC, PM<sub>10</sub>, PM<sub>2.5</sub> and NMVOC in 2014 and 2015.  
880 Additionally, OEA has a significant emission increment for NMVOC (30%), OC (143%), PM<sub>10</sub>  
881 (52%) and PM<sub>2.5</sub> (81%) when taking biomass burning into account. Given the large contributions  
882 to ozone and climate change from NMVOC, CO and aerosols, it's important to address the open  
883 biomass burning contributions in designing mitigation strategies for these areas.

884 In a global context, Asia shares out 43%~56% of the global anthropogenic emissions in 2017,  
885 including 44% for NO<sub>x</sub>, 43% for SO<sub>2</sub>, 49% for CO<sub>2</sub>, 51% for NH<sub>3</sub>, 55% for CO, 50% for  
886 NMVOC, and over 50% for all PM species, **Emissions over Asia are derived from MIXv2, and**  
887 **emissions over the rest of the world are estimated by EDGARv6.** Figure S1 depicts the emissions  
888 trend by Asian regions, United States and OECD-Europe from anthropogenic sources. Asia is  
889 playing a more and more important role in global climate change as its CO<sub>2</sub> emission fraction has

Deleted: 1

Deleted: 3

Deleted: 3

Deleted: (MIX for Asia, EDGAR for other regions)

894 increased by 7% during 2010-2017. Especially, with the general emission reductions in the U.S.  
895 and OECD-Europe, India and Southeast Asia is catching up with the emissions of these two  
896 developed regions for NO<sub>x</sub>, SO<sub>2</sub> and CO<sub>2</sub>, and already surpassed their emissions for other  
897 species. As of now, U.S. and OECD-Europe emissions are in general comparable to those of  
898 OSA for most air pollutants.

899

### 900 3.2 Emissions evolution from 2010–2017

901 For anthropogenic sources, driven by stringent air pollution control measures implemented over  
902 China and OEA since 2010, Asian emissions have declined rapidly by 24.3% for SO<sub>2</sub>, 16.6% for  
903 CO, 17.2% for PM<sub>10</sub>, 18.7% for PM<sub>2.5</sub>, 14.2% for BC and 19.8% for OC, according to our  
904 estimates. On the contrary, CO<sub>2</sub>, NMVOC and NH<sub>3</sub> still show emissions increasing continuously,  
905 with growth rates of 16.5%, 12.6%, and 4.4% during 2010-2017, respectively. The emission  
906 changing ratios are summarized in Table 4 and shown in Fig. 3 and Fig. 4. As demonstrated in  
907 Fig. 4, power, industry, residential and transportation contribute to the rapid emission changes. In  
908 contrast to the smoothly changing patterns for anthropogenic, open biomass burning emissions  
909 vary from year to year, peaking in 2015 as a result of El Niño (Field et al., 2016). Open fire  
910 activities dominate the SEA emission changes for CO, OC, NMVOC, PM<sub>10</sub> and primary PM<sub>2.5</sub>  
911 (see Fig. 3). Marked reductions are estimated for China, with a concurrent increase over India  
912 and Southeast Asia for all species except CO<sub>2</sub>, NMVOC and NH<sub>3</sub> (see Fig. 5). Consequently, air  
913 pollutants, including ozone and secondary aerosol precursors of NO<sub>x</sub>, have shifted southward  
914 (Zhang et al., 2016). This changing spatial pattern has been confirmed from observations as  
915 described in previous studies (Samset et al., 2019). We illustrate the driving forces of emissions  
916 evolution for each species below. Shipping is not included in the following analyses.

917 **NO<sub>x</sub>.** NO<sub>x</sub> emissions show increasing-decreasing-increasing trend for 2010-2017, with a peak in  
918 2012. This trend is a combination of significant power plant emissions reduction (-22% from  
919 2010-2017), and emissions increase from industry (+4%) and transportation (+6%). As  
920 estimated, China's emissions for all anthropogenic sectors dropped by 4.6 Tg (-17%) from 2010-  
921 2017, along with 2.6 Tg (+38%) emissions growth from India and 0.9 Tg (+19%) from SEA. As  
922 a result, China's contribution decreased from 63% to 54%, and Indian share grew from 16% to  
923 22% (anthropogenic, Fig. 5a). In China, power plant emissions dropped by 4.5 Tg (-51%)  
924 because very stringent emission standards are implemented for power plants since 2003, which  
925 has continuous substantial impacts on SO<sub>2</sub>, NO<sub>x</sub> and particulate matters (Chinese National  
926 Standards GB 13223-2003 and 3223-2011) (Zheng et al., 2018). Furthermore, "Ultra-low"  
927 emission standards were set up by the Chinese government in 2015 to further reduce emissions  
928 from coal-fired power plants by 60% by 2020. OEA shows 21% emissions decrease because of  
929 continuous control measures over industry (-16%) and transportation (-32%). Due to insufficient  
930 control strategies in India, OSA and SEA, NO<sub>x</sub> anthropogenic emissions have grown by 38%,  
931 18% and 19%, respectively, mainly driven by power plants and vehicle growth (see Fig. 5a).  
932 Open biomass burning has limited effect (~11%) on NO<sub>x</sub> emissions over SEA and is neglectable  
933 for other regions (<3%).

934 **SO<sub>2</sub>.** SO<sub>2</sub> emissions rapidly declined from 43.8 Tg to 33.1 Tg during 2010-2017, peaking in  
935 2012. Significant reductions of industrial SO<sub>2</sub> emissions (-8.7 Tg, -39%) lead to the marked total  
936 emissions decrease (see Fig. 4). China's emissions dropped by 62%, partly offset by the  
937 concurrent emissions increase of India (+46%) and Southeast Asia (+41%). Stringent control  
938 measures shutting down small industrial boilers and cleaning larger ones in China are the  
939 primary driving forces (Zheng et al., 2018). New emissions standards were set up for coal-fired  
940 industrial boilers with tightened SO<sub>2</sub> limit values (Zheng et al., 2018). In addition, nationwide

Deleted: 3

Deleted:

Deleted: trends

Deleted: P

Deleted: s

Deleted: are the major driving factor for emissions reduction of NO<sub>x</sub> (-3.5% from 2010-2017) during the investigated period. As illustrated by Zheng et al. (2018), China has implemented

950 phasing out of outdated industrial capacity and small, polluting units has been carried out in  
951 China since 2013. Consequently, China's emission fraction decreases from 64% to 32%, ranking  
952 2<sup>nd</sup> in 2017. India's proportion grew from 22% to 41%, and nowadays it's the largest SO<sub>2</sub> emitter  
953 in Asia (anthropogenic, see Fig. 5b). Relatively small emission changes are estimated for OEA (-  
954 0.2 Tg) and OSA (+0.6 Tg). Significant emissions growth from power plants drives the total  
955 anthropogenic increase by 44%, and a 41% rise when considering additional open biomass  
956 burning for SEA.

957 **CO.** Anthropogenic CO shows moderate emissions reduction (-16%) since 2010, driven by the  
958 clean air actions implemented in China covering industry (-38% changes), residential (-20%) and  
959 transportation (-22%). Based on the index decomposition analysis, the improvements in  
960 combustion efficiency and oxygen blast furnace gas recycling in industrial boilers are the largest  
961 contributors to the emission reductions in China (Zheng et al., 2018). Replacing polluted fuel  
962 (biofuel, coal) with cleaner fuels (natural gas, electricity) is the primary driving force in the  
963 residential sector. Despite the rapid vehicle growth which would typically yield a CO increase,  
964 pollution control measures reduced the net CO emission factors by fleet turnover with cleaner  
965 models replacing the older, more polluted vehicles in the market. OEA shows emission  
966 reductions in industry (-37%), residential (-22%) and transportation (-28%). Residential fuel  
967 combustion decreases by 20% and 11% for SEA and India, respectively, having a canceling  
968 effect on the total emissions growth for these two regions. Open biomass burning accounts for  
969 25% ~ 77% of CO emissions in SEA, which drives the total emissions reduction by 19% in 2017  
970 compared to 2010. Additionally, the climate anomaly due to El Niño in 2015 leads to the rapidly  
971 CO emissions drop from 2015 to 2016 in SEA.

972 **CO<sub>2</sub>.** Driven by economic and population growth, anthropogenic CO<sub>2</sub> emissions show a rapid  
973 increasing trend for China (15%), India (32%), OSA (32%) and SEA (21%). We found slight  
974 emission decreases for OEA (-2%). Power, industry, and transportation grew by 28%, 12% and  
975 35%, respectively, driving the total emissions increase continuously. In contrast, we estimate a  
976 5% CO<sub>2</sub> emission reduction from the residential sector, attributed to reduced fuel combustion.  
977 Notable emissions have increased for sectors apart from residential for India (increasing rates  
978 varying between 39% ~ 57%), OSA (43% ~ 56%), and SEA (9% ~ 48%). Fractions by regions  
979 are stable during the studied period, with 62% contribution from China, 8% from OEA, 16%  
980 from India, 3% from OSA, and 11% from SEA (see Fig. 3). Open biomass burning curbs the  
981 total emission growth in SEA from +21% to +5%.

982 **NM VOC.** Differing from the decreasing emission trend for NO<sub>x</sub>, SO<sub>2</sub> and CO, NMVOC  
983 increases by 13% for anthropogenic, and 6% for all sources with open biomass burning. In  
984 China, the industrial sector (+5.1Tg, +35%) is the major reason for the emissions growth, and  
985 industrial solvent use (e.g., architecture paint use, wood paint use) is the largest contributor. The  
986 share of solvent use rapidly rises from 28% in 2010 to 42% in 2017. In addition, oil production,  
987 distribution and refineries, and chemical production lead to a corresponding emissions increase  
988 by 44% (Li et al., 2019b). Due to fuel transfer in residential stoves and the effective pollution  
989 control measures for on-road vehicles, China shows 18% and 22% emissions decreases,  
990 respectively, slowing down the increasing trend. Industry and transportation drive the  
991 anthropogenic emissions in India and SEA growing by 18% and 13%, respectively (see Fig. 5c).

Deleted: d

Deleted: fossil fuel

Deleted: use

995 In SEA, 64% of the total emissions are contributed by open biomass burning in 2015. Compared  
 996 to 2010, 2017 total emissions decreased by 12% in SEA, attributed to biomass burning.  
 997 NMVOCs are speciated into three chemical mechanisms following the source-profile based  
 998 methodology (see Sect. 2.4). We analyzed the speciation results in Sect. 3.5.

999 **NH<sub>3</sub>**. As estimated by MIXv2, NH<sub>3</sub> emissions are generally flat, with slight increases (+4%) over  
 1000 Asia due to the lack of targeted control measures. Over 80% of the total emissions are  
 1001 contributed by fertilizer application and livestock manure. Transportation emissions in 2017 are  
 1002 2.8 times greater than those in 2010 due to vehicle growth, which can play a key role for urban  
 1003 air quality. India is the largest contributor (35%), followed by China (32%) and SEA (17%) (see  
 1004 Fig. 3). India and OSA emissions show monotonic 7% and 20% increases, respectively.  
 1005 According to our estimates, China decreases by 8% reflecting the agricultural activity rate  
 1006 changes. Limited effects are estimated from open fires over NH<sub>3</sub> emissions budget, peaking at  
 1007 19% of the total in 2015 for SEA.

1008 **Particulate Matter (PM)**. PM emissions are estimated to have decreased in Asia: -4.9 Tg PM<sub>10</sub> (-  
 1009 17%), -3.8 Tg PM<sub>2.5</sub> (-19%), -0.45 Tg BC (-14%), -1.3 Tg OC (-20%) for anthropogenic, and -  
 1010 6.5 Tg PM<sub>10</sub> (-20%), -5.0 PM<sub>2.5</sub> (-21%), -0.51 Tg BC (-15%), -1.9 Tg OC (-23%) after including  
 1011 open biomass burning. Industrial and residential sectors are the primary driving forces of the  
 1012 emissions reduction. In China, the strengthened particulates standard for all emission-intensive  
 1013 industrial activities, including iron and steel making, cement, brick, coke, glass, chemicals, and  
 1014 coal boilers have driven the technology renewal and the phasing out of outdated, highly polluting  
 1015 small facilities (Zheng et al., 2018). Pollution control measures reduced power plant emissions  
 1016 by ~30% for PM<sub>10</sub>, PM<sub>2.5</sub> and BC, and counterbalanced the transportation emissions despite  
 1017 vehicle ownership increasing by 270% in seven years. Other East Asia shows significant  
 1018 anthropogenic emissions reduction for all PM species: -32% for PM<sub>10</sub>, -33% for PM<sub>2.5</sub>, -27% for  
 1019 BC, and -31% for OC. Flat trends are estimated in India for all PM species (±8%). Reduction in  
 1020 biofuel fuel use led to the residential emission reduction of PM in India and SEA. Increasing  
 1021 industrial activities led to 24% - 35% anthropogenic emissions growth for PM<sub>10</sub> and PM<sub>2.5</sub> in  
 1022 OSA. As a result, China's emission fractions are shrinking, with growing contributions from  
 1023 India and OSA (see Fig. 5d). Taking PM<sub>2.5</sub> as an example, the emissions shares among Asian  
 1024 regions have changed significantly between 2010 and 2017: from 58% to 46% for China, 23% to  
 1025 30% for India, and 12% to 14% for SEA (anthropogenic, Fig. 5d). Open biomass burning  
 1026 dominates the SEA emissions changes between 2010-2017: -19% for PM<sub>10</sub>, -24% for PM<sub>2.5</sub>, -  
 1027 20% for BC, and -30% for OC.

1028

Deleted: T

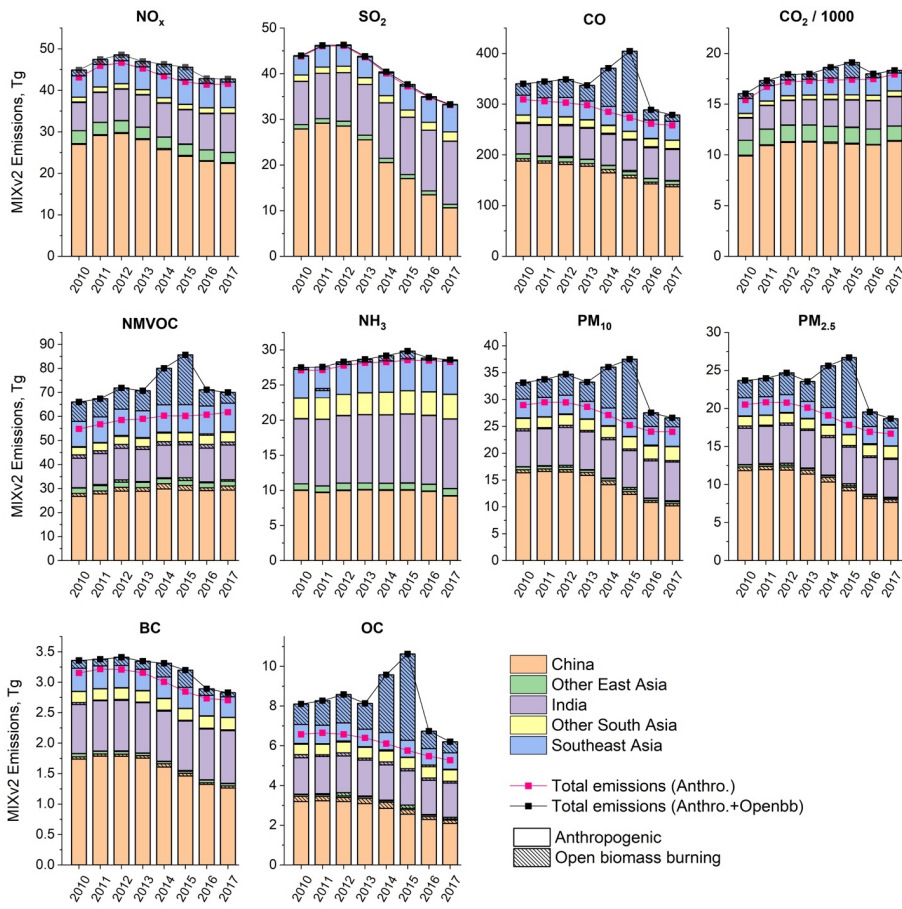
Deleted: in China

Deleted: Reduction in fossil fuel use led to the residential emission reduction of PM in China, India, and SEA.

Deleted: In China, p

Deleted: for anthropogenic sectors

Deleted: trend



1036  
 1037  
 1038  
 1039

**Figure 3. Emission changes by countries / regions from 2010 – 2017. Shares of open biomass burning for each region are shown as shadowed blocks.**

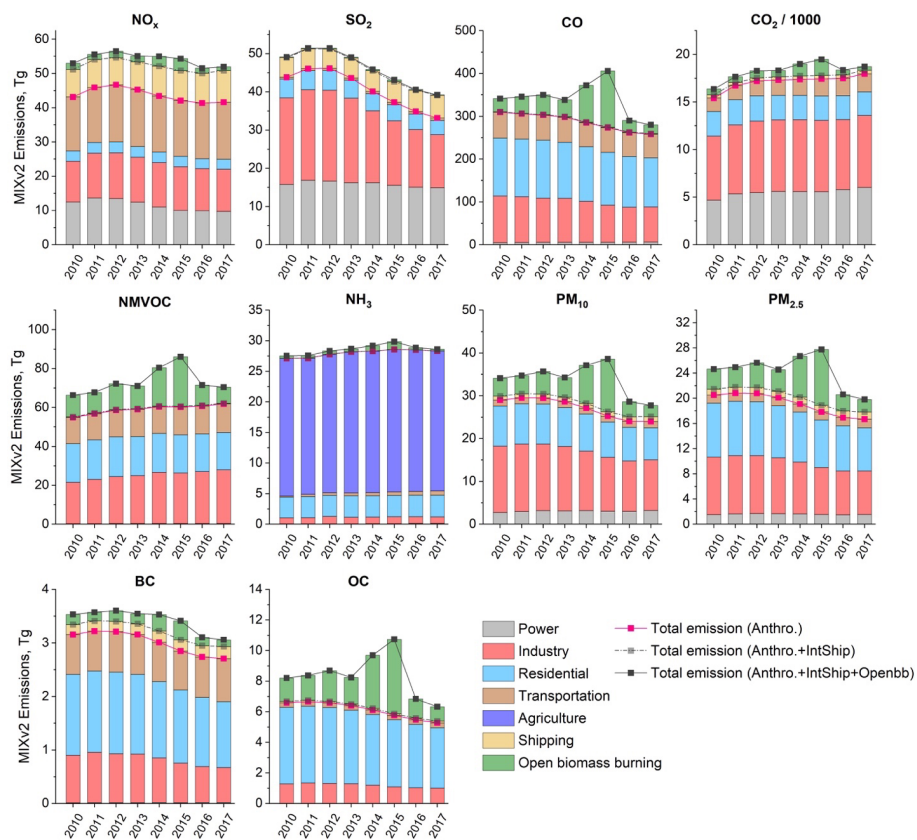


Figure 4. Emission changes by sectors in Asia from 2010 – 2017.

1040  
 1041  
 1042  
 1043  
 1044  
 1045  
 1046  
 1047  
 1048



1049



1050

1051

1052

1053

1054

1055

**Figure 5. Emission changes for anthropogenic sources (power, industry, residential, and transportation) by regions and sectors from 2010 – 2017 for (a) NO<sub>x</sub>, (b) SO<sub>2</sub>, (c) NMVOC and (d) PM<sub>2.5</sub>. The pie sizes are scaled with the total anthropogenic emissions in Asia. The unit for the total emission values in the center is Tg per year. OEA denotes East Asia other than China, OSA represents South Asia other than India, SEA is Southeast Asia.**

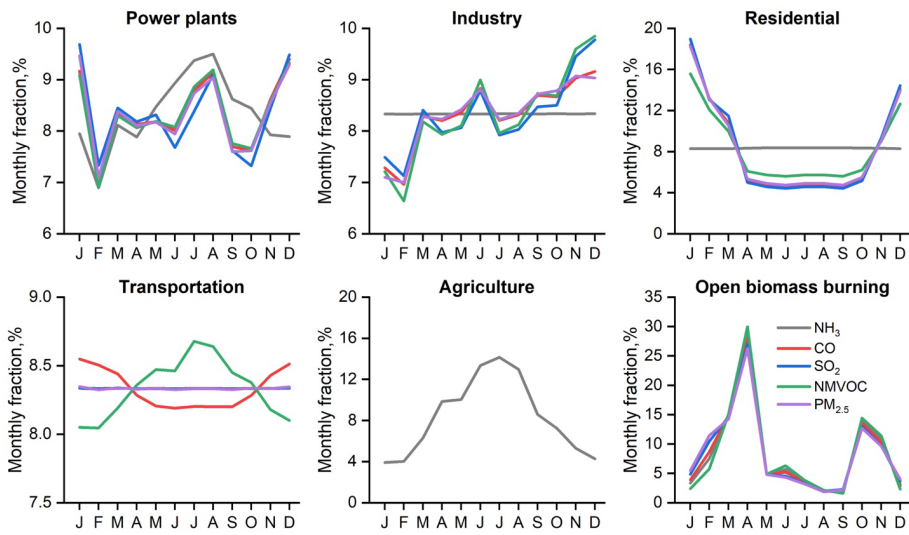
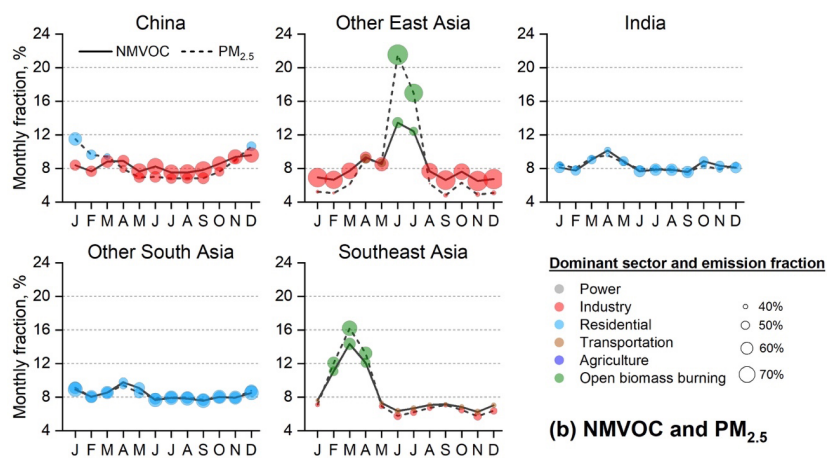
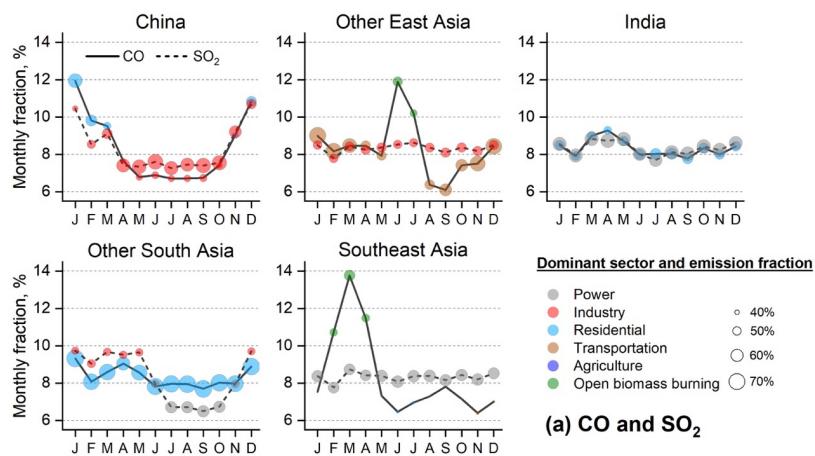


Figure 6. Monthly variations of emissions in Asia by sectors, 2017. For agriculture, only NH<sub>3</sub> emissions are estimated.

1056  
1057  
1058



1059

1060 **Figure 7. Monthly variations of emissions in Asian regions in 2017 for (a) CO (solid lines)**  
 1061 **and SO<sub>2</sub> (short, dashed lines), (b) NMVOC (solid lines) and PM<sub>2.5</sub> (short, dashed lines).**  
 1062 **For each month, the dominant sector is labeled by circle color. Circle area is scaled based on**  
 1063 **the emission fraction of the dominant sector for each month. Both anthropogenic and open**  
 1064 **biomass burning are included.**

### 1065 3.3 Seasonality

1066 Monthly variations of emissions, which are highly sector dependent, are estimated in MIXv2,  
1067 which are highly sector dependent. Within the same sector, similar monthly emission variations  
1068 are found among different species as they are mainly driven by activity rates (see Fig. 6) (Li et  
1069 al., 2017c). Fig. 6 and Fig. 7 illustrate the emission fractions by sectors, and the dominant sector  
1070 (classified by circle color) for each month for CO, SO<sub>2</sub>, NMVOC and PM<sub>2.5</sub> by regions in 2017,  
1071 including both anthropogenic and open biomass burning. Contribution of the “dominant sector”  
1072 is scaled to the circle area. Large circles represent the significant role of the dominant sector and  
1073 small ones (near 17%) indicate the balanced contribution from six sectors. The monthly  
1074 emissions patterns show large disparities varying with regions. Notable variations are estimated  
1075 for emissions of China, OEA and SEA. The residential sector of China is the largest contributor  
1076 in winter for CO and PM<sub>2.5</sub>, leading to the “valley” curves. Industrial emissions show relatively  
1077 high fractions in the second half of the year aiming to achieve the annual production goal, which  
1078 dominate the seasonal patterns of SO<sub>2</sub>, CO, NMVOC and PM<sub>2.5</sub> for most of the months. The  
1079 emissions peak in summer for OEA and March for SEA are attributed to significant in-field  
1080 biomass burning activities. Indian and OSA emissions show relatively small monthly variations,  
1081 compared to other Asian regions. This pattern is attributed to the predominant role of the  
1082 residential sector on the monthly emissions for the investigated species (as illustrated in Fig. 7).  
1083 The minimal seasonal variations in surface temperature within the tropical climate of India and  
1084 OSA contribute to the overall stability in monthly residential emission patterns. Thus, it’s  
1085 important to take both anthropogenic and open biomass sectors into account in seasonality  
1086 analyses given their dominant roles varying by months, such as model evaluations based on  
1087 ground/satellite/aircraft measurements.

1088

### 1089 3.4 Spatial distribution

1090 Gridded emissions at 0.1 × 0.1 degree were developed in our inventory. Power plant emissions in  
1091 China and India are developed on a unit basis and assigned with exact geophysical locations. For  
1092 other sources, emissions are allocated to grids based on spatial proxies, such as road map,  
1093 population, Gross Domestic Product (GDP), etc. The gridded MODIS fire product with high  
1094 spatial resolution (up to 1km) is the essential dataset for open biomass burning emission  
1095 estimation. Fig. 8 and Fig. 9 depict the spatial distribution of both CO<sub>2</sub> and air pollutants over  
1096 Asia in 2017, showing the distinct patterns of point source, roads, and city clusters. Emission  
1097 intensities of hot spots over the Indo-Gangetic Plain, spanning northern Pakistan, northern India  
1098 and Bangladesh are comparable to those of northern China and Indonesia, especially for NH<sub>3</sub>,  
1099 NMVOC, BC and OC. Clear shipping routes can be seen for NO<sub>x</sub>, SO<sub>2</sub>, CO<sub>2</sub> and PM species.

1100 Emission reductions in East Asia highlight the importance of air pollution control in Southern  
1101 Asia. We show the emission changes by latitude bands from 2010 to 2017 for ozone precursors  
1102 (NO<sub>x</sub>, NMVOC, CO) and primary PM<sub>2.5</sub> in Fig. 10 and Fig. S2 (featuring open biomass burning).  
1103 Largest reductions are estimated between 35°N ~ 40°N for NO<sub>x</sub> (-25%), CO (-32%) and PM<sub>2.5</sub> (-  
1104 35%) because of China’s effective emission control strategies. On the other hand, NO<sub>x</sub>

Deleted: s

Deleted: ure

Deleted: ure

Deleted: emissions

Deleted: .

1110 anthropogenic emissions have increased by 15% over 10°S ~ 0° (Southeast Asia), and +27%  
1111 over 10°N ~ 20°N (driven by India). Open biomass burning enlarged the emission amplitude for  
1112 15°S ~ 0° (Southeast Asia), while had limited effect on the trends over other latitude bands (see  
1113 [Fig. S2](#)). To conclude, NO<sub>x</sub> has shifted southward in Asia. NMVOC emissions show generally  
1114 increasing trend over all latitude bands (+5% ~ +38%, anthropogenic). Differently, CO and  
1115 primary PM<sub>2.5</sub> show general emissions reduction since 2010 except over 15°S ~ 10°S and 10°N ~  
1116 20°N. These latitudinal shifts are of particular importance for the global tropospheric ozone  
1117 budget as ozone precursors emitted at low latitudes are more efficient at producing ozone than if  
1118 the same quantity of emissions is released at high latitudes (Zhang et al., 2016; Zhang et al.,  
1119 2021).

Deleted: ure

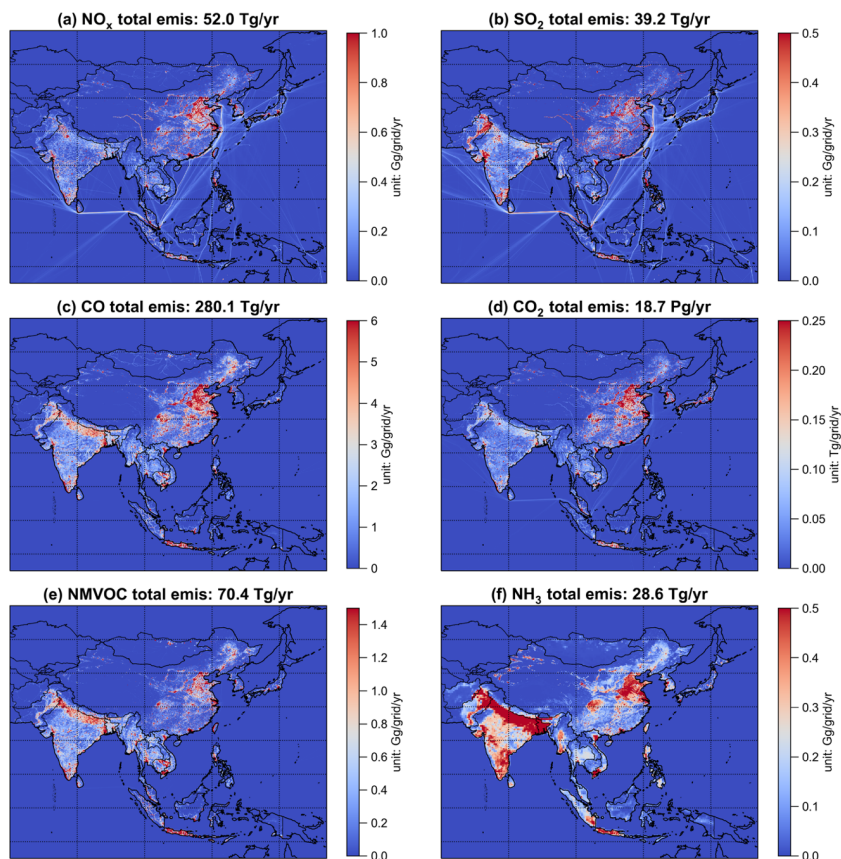


Figure 8. Spatial distribution of emissions in MIXv2 in 2017 for gaseous species.

1121  
1122  
1123  
1124

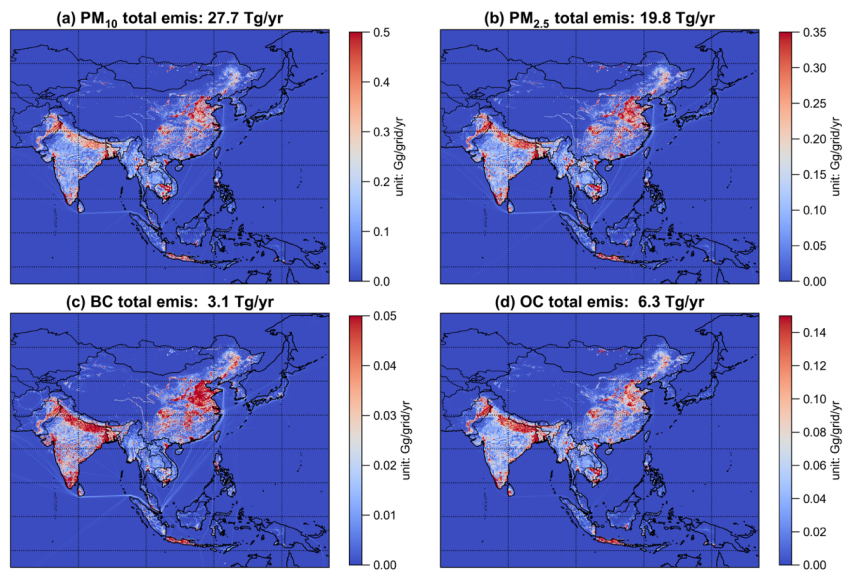
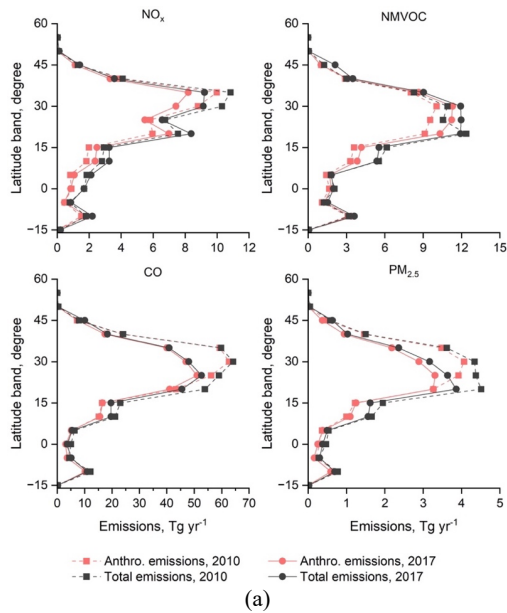


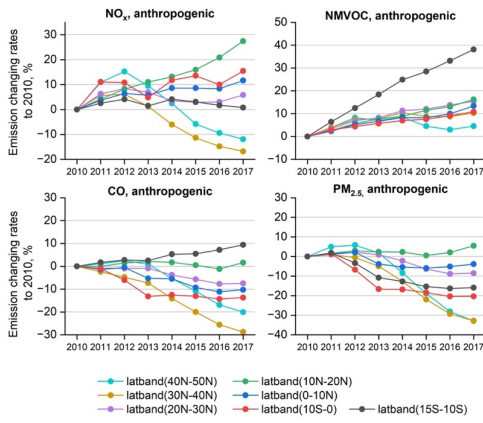
Figure 9. Spatial distribution of emissions in MIXv2 in 2017 for PM species.

1125  
1126  
1127





(a)



(b)

1128  
1129  
1130

1131  
1132  
1133  
1134

**Figure 10. Emissions in 2010 and 2017 (a), and anthropogenic emission changes from 2010 to 2017 (b) by latitude bands for NO<sub>x</sub>, NMVOC, CO and PM<sub>2.5</sub>. The total emissions**

1135 changing patterns by latitude (anthropogenic + open biomass burning) are shown in Figure  
1136 S2.

Deleted: trend

Deleted: B

1137

### 1138 3.5 Speciated NMVOC emissions

1139 As one of the key precursors of ozone and secondary organic aerosols (SOA), NMVOC gain  
1140 more and more attention because of the emission increase due to relatively loose targeted control  
1141 measures. As estimated in MIXv2, Asian emissions have increased by 13% for anthropogenic  
1142 sources and 6% with additional open biomass burning. We speciated the total NMVOC to three  
1143 chemical mechanisms: SARPC99, SAPRC07 and CB05 following the profile-based approach  
1144 (Sect. 2.5). Emission changes during 2010-2017 by chemical groups are shown in Fig. 11.  
1145 Alkanes, Alkenes and Aromatics comprise 78% of the total emissions on a mole basis in 2017.  
1146 Driven by the growing activities in industry, emissions of Alkanes and Aromatics increased by  
1147 ~20% within 7 years, according to our estimates. Alkenes and Alkynes show a stable trend,  
1148 reflecting the combined results of emission reduction in residential and growth in industry and  
1149 transportation sectors. For OVOCs, especially Aldehydes, emissions decreased by 10% since  
1150 2010 due to reduced residential fuel combustion. Open biomass burning play a role over other  
1151 OVOCs (OVOCs other than Aldehydes and Ketones) emission changes. India, Southeast Asia,  
1152 and China are the largest contributors to the total Asian budget, with varying sector distributions  
1153 and driving forces by chemical groups.

Deleted: flat

Deleted:

Deleted: as

Deleted: , compensated by

1154 Industry, mainly industrial solvent use, is the primary driving sector for emissions increase of  
1155 Alkanes (+15%) and Aromatics (+21%) in China. Moderate reductions are estimated for  
1156 anthropogenic OVOCs (-33% Aldehydes, +20% Ketones, -22% other OVOCs) attributed to fuel  
1157 transfer in the residential sector. OEA emissions show generally decreasing trends from -13%  
1158 (Ketones, Alkenes) to +3% (Alkynes) for anthropogenic sectors, and -10% (Ketones, Aromatics,  
1159 Others) to +25% (Other OVOCs) with additional open biomass burning. Industrial emissions  
1160 have decreased over all chemical groups for OEA. Similar sectoral distributions across chemical  
1161 species are found for India and OSA, dominated by the residential and transportation sectors.  
1162 More than 29% emissions growth are estimated for Alkanes and Aromatics, driven by industry,  
1163 residential, and transportation sectors in India and OSA. In SEA, ~20% increases are estimated  
1164 for emissions of Alkanes and Aromatics, and minor changes for Alkenes, Alkynes, Aldehydes  
1165 and Ketones (within 10%) during 2010-2017. OVOCs emissions in 2017 are 25% lower than the  
1166 values in 2010, contributed by residential sources and open biomass burning.

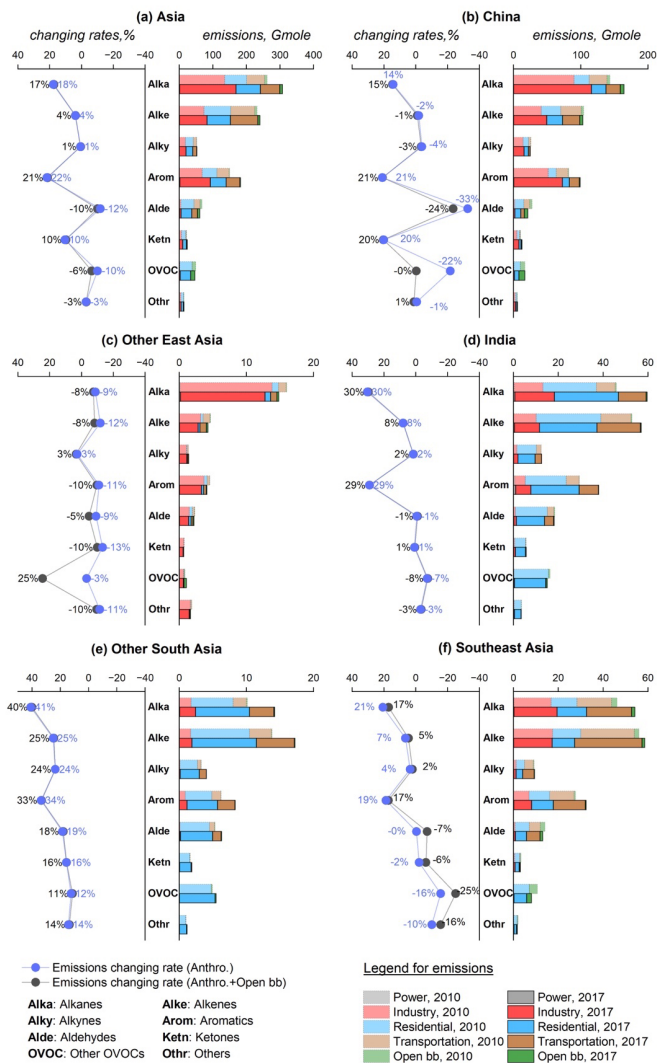
1167

1168

1169

1170

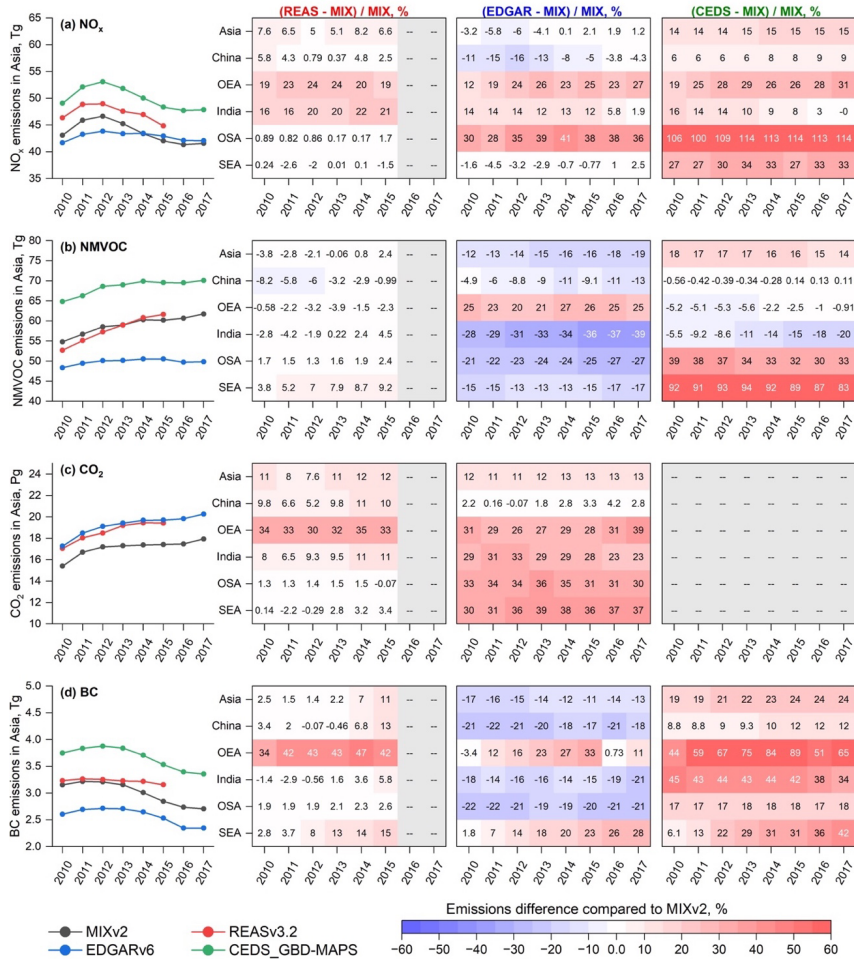
1171



1178  
1179  
1180

**Figure 11. Emissions in 2010 and 2017 (right columns) and the emission changing rates from 2010–2017 (left columns) of NMVOCs by chemical groups. For each country/region,**

1181 the left column represents the emission changing rates (in unit of %), and the right column  
 1182 shows the emissions by sectors in 2010 and 2017. Chemical groups are lumped from the  
 1183 SAPRC07 species following Table S3. Open bb denotes open biomass burning.



1184  
 1185 **Figure 12. Emission comparisons for anthropogenic sources between MIXv2, REASv3.2,**  
 1186 **EDGARv6, and CEDS\_GBD-MAPS for (a) NO<sub>x</sub>, (b) NMVOC, (c) CO<sub>2</sub> and (d) BC during**  
 1187 **2010–2017 by Asian regions.**

1188 **4. Inter-comparisons with other bottom-up and top-down emission**  
 1189 **estimates**

1190

1191

**Table 5. Top-down emission trends since 2010 over Asia.**

Deleted: 4

Species	Estimates	Region	Period	AGR (% yr <sup>-1</sup> ) <sup>a</sup>	Techniques
NO <sub>x</sub>	Krotkov et al. (2016)	E China	2010-2015	-4.9	Satellite
	Liu et al. (2016)	E China	2010-2015	-5.1	Satellite
	Miyazaki et al. (2017)	China	2010-2016	-2.6	Inverse Modeling
	van der A et al. (2017)	E China	2010-2015	-1.7	Inverse Modeling
	Georgoulias et al. (2019)	China	2011-2018	-6.2	Satellite
	Hou et al. (2019)	China	2010-2017	-4.1	Satellite
	Itahashi et al. (2019)	China	2010-2016	-1.6	Inverse Modeling
	Zhang et al. (2019)	China	2010-2017	-5.0	Satellite
	MIXv2	China	2010-2017	-2.6	Bottom-up
	Krotkov et al. (2016)	India	2010-2015	3.4	Satellite
Miyazaki et al. (2017)	India	2010-2016	2.5	Inverse Modeling	
Itahashi et al. (2019)	India	2010-2016	6.0	Inverse Modeling	
MIXv2	India	2010-2017	4.7	Bottom-up	
SO <sub>2</sub>	Tropospheric Chemistry Reanalysis (TCR-2) <sup>b</sup>	China	2010-2017	-7.1	Inverse Modeling
	Krotkov et al. (2016)	E China	2010-2015	-11.0	Satellite
	van der A et al. (2017)	E China	2010-2015	-8.0	Inverse Modeling
	C. Li et al. (2017)	China	2010-2016	-18.0	Inverse Modeling
	Koukouli et al. (2018)	China	2010-2015	-6.2	Inverse Modeling
	Zhang et al. (2019)	China	2010-2017	-4.0	Satellite
	Qu et al. (2019) <sup>c</sup>	China	2010-2017	-4.0	Inverse Modeling
	MIXv2	China	2010-2017	-12.9	Bottom-up
	TCR-2 <sup>b</sup>	India	2010-2017	1.2	Inverse Modeling
	Krotkov et al. (2016)	India	2010-2015	6.0	Satellite
	C. Li et al. (2017)	India	2010-2016	3.4	Inverse Modeling
	Qu et al. (2019) <sup>c</sup>	India	2010-2017	1.7	Inverse Modeling
	MIXv2	India	2010-2017	5.6	Bottom-up
CO	Jiang et al. (2017) <sup>d</sup>	China	2010-2015	-2.8	Inverse Modeling
	Zheng et al. (2019) <sup>e</sup>	China	2010-2017	-2.1	Inverse Modeling
	MIX v2	China	2010-2017	-4.4	Bottom-up
	Jiang et al. (2017) <sup>d</sup>	India / SEA	2010-2015	2.9	Inverse Modeling

	Zheng et al. (2019)	India	2010-2017	-1.7	Inverse Modeling
	MIXv2	India	2010-2017	0.4	Bottom-up
	Zheng et al. (2019)	SEA (an) <sup>f</sup>	2010-2017	-2.4	Inverse Modeling
	MIXv2	SEA (an)	2010-2017	-0.8	Bottom-up
	Jiang et al. (2017)	SEA (bb) <sup>g</sup>	2010-2014 [2010-2015] <sup>h</sup>	6.3 [51.6] <sup>h</sup>	Inverse Modeling
	Zheng et al. (2019)	SEA (bb)	2010-2017 [2010-2015]	-11.2 [40.1]	Inverse Modeling
	MIXv2	SEA (bb)	2010-2017 [2010-2015]	-7.9 [40.1]	Bottom-up
NMVO C	Stavrakou et al. (2017)	China	2010-2014	1.7	Inverse Modeling <sup>i</sup>
	Zhang et al. (2019)	China	2010-2017	1.0	Satellite <sup>i</sup>
	MIXv2	China	2010-2017	1.3	Bottom-up
NH <sub>3</sub>	Warner et al. (2017)	China	2010-2016	2.2	Satellite
	Damme et al. (2021)	China	2010-2017	5.5	Satellite
	MIXv2	China	2010-2017	-1.2	Bottom-up
	Damme et al. (2021)	India	2010-2017	0.5	Satellite
	MIXv2	India	2010-2017	2.2	Bottom-up
	Damme et al. (2021)	SEA	2010-2017 [2010-2015]	-2.7 [8.9]	Satellite
	MIXv2	SEA	2010-2017 [2010-2015]	1.7 [5.3]	Bottom-up

1193

1194 <sup>a</sup> AGR: Annual Growth Rate.

1195 <sup>b</sup> Elguindi et al. (2020)

1196 <sup>c</sup> Top-down estimates based on NASA products

1197 <sup>d</sup> estimates derived from MOPITT profiles

1198 <sup>e</sup> the results of full inversion # 3 are summarized here

1199 <sup>f</sup> Southeast Asia for anthropogenic sources

1200 <sup>g</sup> Southeast Asia for open biomass burning

1201 <sup>h</sup> the growth rates between 2010 and 2015 are listed in square brackets because 2015 is a El Niño year

1202 <sup>i</sup> HCHO columns are used

1203

1204 To provide a potential uncertainty range of MIXv2, we compared our estimates with both  
 1205 regional and global inventories, as well as top-down estimates from previous satellite-based and  
 1206 inverse modeling studies. Figure 12 shows the emission comparisons of MIXv2 with REASv3.2,  
 1207 EDGARv6, and CEDS\_GBD-MAPS (referred to as CEDS) (McDuffie et al., 2020) by Asian  
 1208 regions during 2010-2017 for NO<sub>x</sub>, NMVOC, CO<sub>2</sub> and BC. REAS and MIX show the best  
 1209 agreement (differing within 12%) as expected because REAS was used as default estimates over  
 1210 Asia. Similar trends are found between REAS and MIX for all species except BC. The trends of  
 1211 NO<sub>x</sub> in EDGAR are different than the others which peak in 2012, indicating the needs of re-  
 1212 visiting the parameterization of control policies in East Asia in the global inventory system.

1213 EDGAR estimates are within 20% difference with MIX<sub>v2</sub> for the whole Asia, but with higher  
1214 discrepancies over OEA, OSA and SEA. NMVOCs are 12%~19% lower in EDGAR, mainly for  
1215 India and OSA. Notably, the emission discrepancies have grown larger in recent years, attributed  
1216 to the differences in emissions trends. EDGAR's NMVOC emissions show a relatively flat trend,  
1217 in contrast to the continuously increasing pattern of MIX. Emissions of CO<sub>2</sub> over OEA, OSA and  
1218 SEA seem to be uncertain, with more than 30% difference between EDGAR and MIX. Similarly,  
1219 the emission differences of BC in SEA need to be **considered** when used in climate model  
1220 simulations. The emission trends of CEDS are consistent with those of MIX because MEIC was  
1221 applied to scale the emissions in the CEDS system (McDuffie et al., 2020). However, compared  
1222 to MIX, CEDS emissions are generally higher across regions and species, with large  
1223 discrepancies over OEA (+65% for BC, +31% for NO<sub>x</sub> in 2017), India (+34% for BC), OSA  
1224 (+114% for NO<sub>x</sub>, +33% for NMVOCs) and SEA (+33% for NO<sub>x</sub>, +83% for NMVOCs, +42% for  
1225 BC). These comparisons highlight the potential uncertainties of bottom-up emission inventories  
1226 over South Asia and Southeast Asia where information is still limited compared to East Asia.  
1227 **More validations and revisions are needed to identify the reasons of the discrepancies and narrow**  
1228 **down the gaps.**

1229 **Table 5** summarizes the top-down emission annual growth rates since 2010 as derived from  
1230 satellite retrievals and inverse modeling studies. MIX trends show high consistency with the top-  
1231 down estimates, especially the inverse modeling results. Decreasing trends since the peak in  
1232 2012 for NO<sub>x</sub> emissions in China are validated from space (Georgoulias et al., 2019; Hou et al.,  
1233 2019; Itahashi et al., 2019; Krotkov et al., 2016; Liu et al., 2016; Miyazaki et al., 2017; van der  
1234 A et al., 2017; Zhang et al., 2019). The annual growth rates derived directly from satellite  
1235 retrievals (-4.1 ~ -6.2 % yr<sup>-1</sup>) are in general larger than those from inverse modeling (-1.6 ~ -  
1236 2.6 % yr<sup>-1</sup>) which jointly account for the air transport and chemical non-linearity. Similar  
1237 declining trends are found from top-down estimates of SO<sub>2</sub> (Elguindi et al., 2020; Koukouli et  
1238 al., 2018; Krotkov et al., 2016; Li et al., 2017a; Qu et al., 2019; van der A et al., 2017; Zhang et  
1239 al., 2019) and CO (Jiang et al., 2017; Zheng et al., 2019) over China. For India, emissions have  
1240 been detected to grow continuously from space for NO<sub>x</sub> and SO<sub>2</sub>, with growth rates consistent  
1241 with the inventory estimation. Slightly increasing trend is detected from space for HCHO in  
1242 China, as an indicator of NMVOC emissions (Stavrakou et al., 2017; Zhang et al., 2019). 2015 is  
1243 an El Niño year, and this climate anomaly turns out to significantly affect the emissions trends of  
1244 CO and NH<sub>3</sub> in SEA (Van Damme et al., 2021). More inverse modeling work by combining  
1245 multiple species are needed for NH<sub>3</sub> over Asia to shed light on the uncertainty range of inventory  
1246 estimation.

1247  
1248  
1249  
1250  
1251

Deleted: increasing

Deleted: s

Deleted: noted

Deleted: and close the gaps between the different sources of estimates

Deleted: 4

1258 **5. Concluding remarks**

1259

1260 In this work, we developed the MIXv2 emission inventory for Asia during 2010-2017 resolved  
1261 with relatively high spatial resolution (0.1°) and temporal resolution (monthly), and detailed  
1262 chemical speciation (SAPRC99, SAPRC07, CB05). MEICv2, PKU-NH<sub>3</sub>, PKU-Biomass, ANL-  
1263 India, CAPSS, JPN are used to represent the best available emission inventories for China, India,  
1264 the Republic of Korea, and Japan, fill-gaped with REASv3 and GFEDv4. Constructing a long-  
1265 term mosaic emission inventory requires substantial international collaborations. MIXv2 was  
1266 developed based on the state-of-the-art updated emission inputs under the framework of MICS-  
1267 Asia Phase IV, and is now ready to feed the atmospheric chemistry models and improve  
1268 chemistry-climate models for long-term analyses. With high spatial resolution up to 0.1°, MIXv2  
1269 is capable of supporting model activities at regional and even local scales. As far as we know,  
1270 MIXv2 is the first mosaic inventory with both anthropogenic and open biomass burning  
1271 estimated by incorporating local emission inventories. Emissions are aggregated to seven sectors  
1272 in MIX: power, industry, residential, transportation, agriculture as anthropogenic sources, along  
1273 with open biomass burning and shipping. With three chemical mechanisms developed using a  
1274 consistent speciation framework, MIXv2 can be used in most of the atmospheric models even for  
1275 those configured with updates on ozone and secondary organic aerosols formation. MIXv2 also  
1276 has CO<sub>2</sub> emissions based on the same emissions model for 9 air pollutants (NO<sub>x</sub>, SO<sub>2</sub>, CO,  
1277 NMVOC, NH<sub>3</sub>, PM<sub>10</sub>, PM<sub>2.5</sub>, BC, OC), providing a consistent dataset for climate-air quality  
1278 nexus research. Gridded monthly emissions are publicly available at  
1279 <https://csl.noaa.gov/groups/csl4/modeldata/data/Li2023/>.

1280 Driving forces of the emission changes during 2010-2017 are investigated based on MIXv2.  
1281 Significant emission reductions from anthropogenic sources are found for SO<sub>2</sub>, CO, PM<sub>10</sub>, PM<sub>2.5</sub>,  
1282 BC, and OC, driven by effective clean air actions conducted over China and Other East Asia.  
1283 India, Other South Asia, and Southeast Asia show continuously increasing emissions trends since  
1284 2010, limiting the emissions reduction for Asia as a whole. On the contrary, NMVOC and NH<sub>3</sub>  
1285 emissions increased or remained flat due to insufficient targeted control measures. Open biomass  
1286 burning is the largest contributor to Southeast Asia for emissions of CO, NMVOC and OC. NO<sub>x</sub>  
1287 emissions have shown clear latitudinal shifts southward in Asia, which is important for global  
1288 tropospheric ozone budget. Our estimated trends are in general consistent with those derived  
1289 from satellite retrievals, especially results from inverse modeling.

1290 Further validation is needed for MIXv2 for better understanding of the data reliability. Inverse  
1291 modeling studies on NMVOC and NH<sub>3</sub> are still limited, partly attributed to the lack of available  
1292 measurement data over Asia. With the launch of the Geostationary Environment Monitoring  
1293 Spectrometer (GEMS) and the availability of hourly retrievals of atmospheric composition, top-  
1294 down constraints on both emissions spatial distributions and temporal variations are now  
1295 possible (Kim et al., 2020) on the scale of Asia. In-situ measurements, aircraft and satellite data  
1296 should be combined with inventory and model simulations to improve emission estimates in the  
1297 future.

Deleted: .

Deleted: and

Deleted: ed



1301

## 1302 **6. Data availability**

1303 MIXv2 gridded monthly emissions data [for both anthropogenic and open biomass burning](#) for  
1304 2010-2017 by 10 species and 7 sectors are available at:  
1305 <https://csl.noaa.gov/groups/csl4/modeldata/data/Li2023/>. [Daily open biomass burning emissions](#)  
1306 [are available upon request.](#)

1307

## 1308 **7. Author contribution**

1309 M. Li, Q. Zhang, J. Kurokawa and J. Woo initiated the research topic. M. Li developed the  
1310 emissions model, conducted the analyses, and prepared the paper. J. Kurokawa, Q. Zhang, J.  
1311 Woo, T. Morikawa, S. Chatani, Z. Lu, Y. Song, G. Geng, H. Hu, J. Kim provided the regional  
1312 emissions data. O. R. Cooper and B. C. McDonald have contributed by providing the computing  
1313 resources and data analyses. All co-authors have contributed with paper revision comments.

1314

## 1315 **8. Competing interests**

1316 At least one of our co-authors are members of the editorial board of ACP. The peer-review  
1317 process was guided by an independent editor, and the authors have also no other competing  
1318 interests to declare.

1319

## 1320 **9. Acknowledgement**

1321

1322 MEIC has been developed and maintained by Tsinghua University, supported by the National  
1323 Key R&D program of China (grant no. 2022YFC3700605). REASv3 has been supported by the  
1324 Environmental Research and Technology Development Fund (grant nos. S-12 and S-20,  
1325 JPMEERF21S12012) of the Environmental Restoration and Conservation Agency of Japan and  
1326 the Japan Society for the Promotion of Science, KAKENHI (grant no. 19K12303). The ANL-  
1327 India emission inventory was partially funded by the National Aeronautics and Space  
1328 Administration (NASA) as part of the Air Quality Applied Sciences Team (AQAST) program  
1329 and by the Office of Biological and Environmental Research of Office of Science in the U.S.  
1330 Department of Energy in support of the Ganges Valley Aerosol Experiment (GVAX). Argonne  
1331 National Laboratory is operated by UChicago Argonne, LLC, under Contract No. DE-AC02-  
1332 06CH11357 with the U.S. Department of Energy. JPN emissions are developed by the  
1333 Environment Research and Technology Development Fund (grant nos. JPMEERF20222001,  
1334 JPMEERF20165001 and JPMEERF20215005) of the Environmental Restoration and

1335 Conservation Agency provided by Ministry of the Environment of Japan, and the FRIEND (Fine  
1336 Particle Research Initiative in East Asia Considering National Differences) project through the  
1337 National Research Foundation of Korea (NRF) funded by the Ministry of Science and ICT (grant  
1338 no. 2020M3G1A1114622).

1339 This compilation of the MIXv2 inventory has been supported by NOAA Cooperative Agreement  
1340 with CIRES, NA17OAR4320101 and NA22OAR4320151. The scientific results and  
1341 conclusions, as well as any views or opinions expressed herein, are those of the authors and do  
1342 not necessarily reflect the views of NOAA or the Department of Commerce.

1343

1344

1345

1346 **References**

1347

- 1348 Adam, M. G., Tran, P. T. M., Bolan, N., and Balasubramanian, R.: Biomass burning-derived  
1349 airborne particulate matter in Southeast Asia: A critical review, *Journal of Hazardous Materials*,  
1350 407, 124760, 2021.
- 1351 Akagi, S. K., Yokelson, R. J., Wiedinmyer, C., Alvarado, M. J., Reid, J. S., Karl, T., Crounse, J.  
1352 D., and Wennberg, P. O.: Emission factors for open and domestic biomass burning for use in  
1353 atmospheric models, *Atmos. Chem. Phys.*, 11, 4039-4072, 2011.
- 1354 Andreae, M. O. and Merlet, P.: Emission of trace gases and aerosols from biomass burning,  
1355 *Global Biogeochemical Cycles*, 15, 955-966, 2001.
- 1356 Anwar, M. N., Shabbir, M., Tahir, E., Iftikhar, M., Saif, H., Tahir, A., Murtaza, M. A., Khokhar,  
1357 M. F., Rehan, M., Aghbashlo, M., Tabatabaei, M., and Nizami, A.-S.: Emerging challenges of air  
1358 pollution and particulate matter in China, India, and Pakistan and mitigating solutions, *Journal of*  
1359 *Hazardous Materials*, 416, 125851, 2021.
- 1360 Carter, W. P. L.: Development of a database for chemical mechanism assignments for volatile  
1361 organic emissions, *Journal of the Air & Waste Management Association*, 65, 1171-1184, 2015.
- 1362 Chatani, S., Shimadera, H., Itahashi, S., and Yamaji, K.: Comprehensive analyses of source  
1363 sensitivities and apportionments of PM<sub>2.5</sub> and ozone over Japan via multiple numerical  
1364 techniques, *Atmos. Chem. Phys.*, 20, 10311-10329, 2020.
- 1365 Chatani, S., Yamaji, K., Sakurai, T., Itahashi, S., Shimadera, H., Kitayama, K., and Hayami, H.:  
1366 Overview of Model Inter-Comparison in Japan's Study for Reference Air Quality Modeling (J-  
1367 STREAM), *Atmosphere*, 9, 19, 2018.
- 1368 Chen, L., Gao, Y., Zhang, M., Fu, J. S., Zhu, J., Liao, H., Li, J., Huang, K., Ge, B., Wang, X.,  
1369 Lam, Y. F., Lin, C. Y., Itahashi, S., Nagashima, T., Kajino, M., Yamaji, K., Wang, Z., and  
1370 Kurokawa, J.: MICS-Asia III: multi-model comparison and evaluation of aerosol over East Asia,  
1371 *Atmos. Chem. Phys.*, 19, 11911-11937, 2019.
- 1372 Crippa, M., Guizzardi, D., Butler, T., Keating, T., Wu, R., Kaminski, J., Kuenen, J., Kurokawa,  
1373 J., Chatani, S., Morikawa, T., Pouliot, G., Racine, J., Moran, M. D., Klimont, Z., Manseau, P.  
1374 M., Mashayekhi, R., Henderson, B. H., Smith, S. J., Suchyta, H., Muntean, M., Solazzo, E.,  
1375 Banja, M., Schaaf, E., Pagani, F., Woo, J. H., Kim, J., Monforti-Ferrario, F., Pisoni, E., Zhang,  
1376 J., Niemi, D., Sassi, M., Ansari, T., and Foley, K.: The HTAP v3 emission mosaic: merging  
1377 regional and global monthly emissions (2000–2018) to support air quality modelling and  
1378 policies, *Earth Syst. Sci. Data*, 15, 2667-2694, 2023.
- 1379 Crippa, M., Guizzardi, D., Muntean, M., Schaaf, E., Dentener, F., van Aardenne, J. A., Monni,  
1380 S., Doering, U., Olivier, J. G. J., Pagliari, V., and Janssens-Maenhout, G.: Gridded emissions of  
1381 air pollutants for the period 1970–2012 within EDGAR v4.3.2, *Earth Syst. Sci. Data*, 10, 1987-  
1382 2013, 2018.

1383 Elguindi, N., Granier, C., Stavrakou, T., Darras, S., Bauwens, M., Cao, H., Chen, C., Denier van  
1384 der Gon, H. A. C., Dubovik, O., Fu, T. M., Henze, D. K., Jiang, Z., Keita, S., Kuenen, J. J. P.,  
1385 Kurokawa, J., Lioussé, C., Miyazaki, K., Müller, J. F., Qu, Z., Solmon, F., and Zheng, B.:  
1386 Intercomparison of Magnitudes and Trends in Anthropogenic Surface Emissions From Bottom-  
1387 Up Inventories, Top-Down Estimates, and Emission Scenarios, *Earth's Future*, 8,  
1388 e2020EF001520, 2020.

1389 Feng, Z., Xu, Y., Kobayashi, K., Dai, L., Zhang, T., Agathokleous, E., Calatayud, V., Paoletti,  
1390 E., Mukherjee, A., Agrawal, M., Park, R. J., Oak, Y. J., and Yue, X.: Ozone pollution threatens  
1391 the production of major staple crops in East Asia, *Nature Food*, 3, 47-56, 2022.

1392 Field, R. D., van der Werf, G. R., Fanin, T., Fetzer, E. J., Fuller, R., Jethva, H., Levy, R.,  
1393 Livesey, N. J., Luo, M., Torres, O., and Worden, H. M.: Indonesian fire activity and smoke  
1394 pollution in 2015 show persistent nonlinear sensitivity to El Niño-induced drought, *Proceedings  
1395 of the National Academy of Sciences*, 113, 9204-9209, 2016.

1396 Fiore, A. M., Naik, V., and Leibensperger, E. M.: Air Quality and Climate Connections, *Journal  
1397 of the Air & Waste Management Association*, 65, 645-685, 2015.

1398 Gao, M., Han, Z., Liu, Z., Li, M., Xin, J., Tao, Z., Li, J., Kang, J. E., Huang, K., Dong, X.,  
1399 Zhuang, B., Li, S., Ge, B., Wu, Q., Cheng, Y., Wang, Y., Lee, H. J., Kim, C. H., Fu, J. S., Wang,  
1400 T., Chin, M., Woo, J. H., Zhang, Q., Wang, Z., and Carmichael, G. R.: Air quality and climate  
1401 change, Topic 3 of the Model Inter-Comparison Study for Asia Phase III (MICS-Asia III) –  
1402 Part I: Overview and model evaluation, *Atmos. Chem. Phys.*, 18, 4859-4884, 2018.

1403 Geng, G., Zheng, Y., Zhang, Q., Xue, T., Zhao, H., Tong, D., Zheng, B., Li, M., Liu, F., Hong,  
1404 C., He, K., and Davis, S. J.: Drivers of PM<sub>2.5</sub> air pollution deaths in China 2002–2017, *Nature  
1405 Geoscience*, 14, 645-650, 2021.

1406 Georgoulias, A. K., van der A, R. J., Stammes, P., Boersma, K. F., and Eskes, H. J.: Trends and  
1407 trend reversal detection in 2 decades of tropospheric NO<sub>2</sub> satellite observations, *Atmos. Chem.  
1408 Phys.*, 19, 6269-6294, 2019.

1409 Hammer, M. S., van Donkelaar, A., Li, C., Lyapustin, A., Sayer, A. M., Hsu, N. C., Levy, R. C.,  
1410 Garay, M. J., Kalashnikova, O. V., Kahn, R. A., Brauer, M., Apte, J. S., Henze, D. K., Zhang, L.,  
1411 Zhang, Q., Ford, B., Pierce, J. R., and Martin, R. V.: Global Estimates and Long-Term Trends of  
1412 Fine Particulate Matter Concentrations (1998–2018), *Environmental Science & Technology*, 54,  
1413 7879-7890, 2020.

1414 Hou, Y., Wang, L., Zhou, Y., Wang, S., Liu, W., and Zhu, J.: Analysis of the tropospheric  
1415 column nitrogen dioxide over China based on satellite observations during 2008–2017,  
1416 *Atmospheric Pollution Research*, 10, 651-655, 2019.

1417 Huang, X., Li, M., Li, J., and Song, Y.: A high-resolution emission inventory of crop burning in  
1418 fields in China based on MODIS Thermal Anomalies/Fire products, *Atmospheric Environment*,  
1419 50, 9-15, 2012a.

1420 Huang, X., Song, Y., Li, M., Li, J., Huo, Q., Cai, X., Zhu, T., Hu, M., and Zhang, H.: A high-  
1421 resolution ammonia emission inventory in China, *Global Biogeochemical Cycles*, 26, 2012b.

1422 Itahashi, S., Ge, B., Sato, K., Fu, J. S., Wang, X., Yamaji, K., Nagashima, T., Li, J., Kajino, M.,  
1423 Liao, H., Zhang, M., Wang, Z., Li, M., Kurokawa, J., Carmichael, G. R., and Wang, Z.: MICS-  
1424 Asia III: overview of model intercomparison and evaluation of acid deposition over Asia, *Atmos.*  
1425 *Chem. Phys.*, 20, 2667-2693, 2020.

1426 Itahashi, S., Yumimoto, K., Kurokawa, J.-i., Morino, Y., Nagashima, T., Miyazaki, K., Maki, T.,  
1427 and Ohara, T.: Inverse estimation of NO<sub>x</sub> emissions over China and India 2005–2016:  
1428 contrasting recent trends and future perspectives, *Environmental Research Letters*, 14, 124020,  
1429 2019.

1430 Jacob, D. J. and Winner, D. A.: Effect of climate change on air quality, *Atmospheric*  
1431 *Environment*, 43, 51-63, 2009.

1432 Janssens-Maenhout, G., Crippa, M., Guizzardi, D., Dentener, F., Muntean, M., Pouliot, G.,  
1433 Keating, T., Zhang, Q., Kurokawa, J., Wankmüller, R., Denier van der Gon, H., Kuenen, J. J. P.,  
1434 Klimont, Z., Frost, G., Darras, S., Koffi, B., and Li, M.: HTAP\_v2.2: a mosaic of regional and  
1435 global emission grid maps for 2008 and 2010 to study hemispheric transport of air pollution,  
1436 *Atmos. Chem. Phys.*, 15, 11411-11432, 2015.

1437 Janssens-Maenhout, G., Crippa, M., Guizzardi, D., Muntean, M., Schaaf, E., Dentener, F.,  
1438 Bergamaschi, P., Pagliari, V., Olivier, J. G. J., Peters, J. A. H. W., van Aardenne, J. A., Monni,  
1439 S., Doering, U., Petrescu, A. M. R., Solazzo, E., and Oreggioni, G. D.: EDGAR v4.3.2 Global  
1440 Atlas of the three major greenhouse gas emissions for the period 1970–2012, *Earth Syst. Sci.*  
1441 *Data*, 11, 959-1002, 2019.

1442 Jiang, Z., Worden, J. R., Worden, H., Deeter, M., Jones, D. B. A., Arellano, A. F., and Henze, D.  
1443 K.: A 15-year record of CO emissions constrained by MOPITT CO observations, *Atmos. Chem.*  
1444 *Phys.*, 17, 4565-4583, 2017.

1445 Kang, Y., Liu, M., Song, Y., Huang, X., Yao, H., Cai, X., Zhang, H., Kang, L., Liu, X., Yan, X.,  
1446 He, H., Zhang, Q., Shao, M., and Zhu, T.: High-resolution ammonia emissions inventories in  
1447 China from 1980 to 2012, *Atmos. Chem. Phys.*, 16, 2043-2058, 2016.

1448 Kim, J., Jeong, U., Ahn, M.-H., Kim, J. H., Park, R. J., Lee, H., Song, C. H., Choi, Y.-S., Lee,  
1449 K.-H., Yoo, J.-M., Jeong, M.-J., Park, S. K., Lee, K.-M., Song, C.-K., Kim, S.-W., Kim, Y. J.,  
1450 Kim, S.-W., Kim, M., Go, S., Liu, X., Chance, K., Chan Miller, C., Al-Saadi, J., Veihelmann, B.,  
1451 Bhartia, P. K., Torres, O., Abad, G. G., Haffner, D. P., Ko, D. H., Lee, S. H., Woo, J.-H., Chong,  
1452 H., Park, S. S., Nicks, D., Choi, W. J., Moon, K.-J., Cho, A., Yoon, J., Kim, S.-k., Hong, H., Lee,  
1453 K., Lee, H., Lee, S., Choi, M., Veeffkind, P., Levelt, P. F., Edwards, D. P., Kang, M., Eo, M.,  
1454 Bak, J., Baek, K., Kwon, H.-A., Yang, J., Park, J., Han, K. M., Kim, B.-R., Shin, H.-W., Choi,  
1455 H., Lee, E., Chong, J., Cha, Y., Koo, J.-H., Irie, H., Hayashida, S., Kasai, Y., Kanaya, Y., Liu,  
1456 C., Lin, J., Crawford, J. H., Carmichael, G. R., Newchurch, M. J., Lefter, B. L., Herman, J. R.,  
1457 Swap, R. J., Lau, A. K. H., Kurosu, T. P., Jaross, G., Ahlers, B., Dobber, M., McElroy, C. T.,  
1458 and Choi, Y.: New Era of Air Quality Monitoring from Space: Geostationary Environment  
1459 Monitoring Spectrometer (GEMS), *Bulletin of the American Meteorological Society*, 101, E1-  
1460 E22, 2020.

1461 Klausbrückner, C., Annegarn, H., Henneman, L. R. F., and Rafaj, P.: A policy review of  
1462 synergies and trade-offs in South African climate change mitigation and air pollution control  
1463 strategies, *Environmental Science & Policy*, 57, 70-78, 2016.

1464 Koukoulis, M. E., Theys, N., Ding, J., Zyrichidou, I., Mijling, B., Balis, D., and van der A, R. J.:  
1465 Updated SO<sub>2</sub> emission estimates over China using OMI/Aura observations, *Atmos. Meas. Tech.*,  
1466 11, 1817-1832, 2018.

1467 Krotkov, N. A., McLinden, C. A., Li, C., Lamsal, L. N., Celarier, E. A., Marchenko, S. V.,  
1468 Swartz, W. H., Bucsela, E. J., Joiner, J., Duncan, B. N., Boersma, K. F., Veefkind, J. P., Levelt,  
1469 P. F., Fioletov, V. E., Dickerson, R. R., He, H., Lu, Z., and Streets, D. G.: Aura OMI  
1470 observations of regional SO<sub>2</sub> and NO<sub>2</sub> pollution changes from 2005 to 2015, *Atmos. Chem.  
1471 Phys.*, 16, 4605-4629, 2016.

1472 Kurokawa, J. and Ohara, T.: Long-term historical trends in air pollutant emissions in Asia:  
1473 Regional Emission inventory in ASia (REAS) version 3, *Atmos. Chem. Phys.*, 20, 12761-12793,  
1474 2020.

1475 Lee, D.-G., Lee, Y.-M., Jang, K.-W., Yoo, C., Kang, K.-H., Lee, J.-H., Jung, S.-W., Park, J.-M.,  
1476 Lee, S.-B., Han, J.-S., Hong, J.-H., and Lee, S.-J.: Korean National Emissions Inventory System  
1477 and 2007 Air Pollutant Emissions, *Asian Journal of Atmospheric Environment*, 5, 278-291,  
1478 2011.

1479 Lei, Y., Zhang, Q., He, K. B., and Streets, D. G.: Primary anthropogenic aerosol emission trends  
1480 for China, 1990–2005, *Atmos. Chem. Phys.*, 11, 931-954, 2011.

1481 Li, C., McLinden, C., Fioletov, V., Krotkov, N., Carn, S., Joiner, J., Streets, D., He, H., Ren, X.,  
1482 Li, Z., and Dickerson, R. R.: India Is Overtaking China as the World's Largest Emitter of  
1483 Anthropogenic Sulfur Dioxide, *Scientific Reports*, 7, 14304, 2017a.

1484 Li, K., Jacob, D. J., Liao, H., Zhu, J., Shah, V., Shen, L., Bates, K. H., Zhang, Q., and Zhai, S.: A  
1485 two-pollutant strategy for improving ozone and particulate air quality in China, *Nature  
1486 Geoscience*, 12, 906-910, 2019a.

1487 Li, M., Klimont, Z., Zhang, Q., Martin, R. V., Zheng, B., Heyes, C., Cofala, J., Zhang, Y., and  
1488 He, K.: Comparison and evaluation of anthropogenic emissions of SO<sub>2</sub> and NO<sub>x</sub> over China,  
1489 *Atmos. Chem. Phys.*, 18, 3433-3456, 2018.

1490 Li, M., Liu, H., Geng, G., Hong, C., Liu, F., Song, Y., Tong, D., Zheng, B., Cui, H., Man, H.,  
1491 Zhang, Q., and He, K.: Anthropogenic emission inventories in China: a review, *National Science  
1492 Review*, 4, 834-866, 2017b.

1493 Li, M., Zhang, Q., Kurokawa, J. I., Woo, J. H., He, K., Lu, Z., Ohara, T., Song, Y., Streets, D.  
1494 G., Carmichael, G. R., Cheng, Y., Hong, C., Huo, H., Jiang, X., Kang, S., Liu, F., Su, H., and  
1495 Zheng, B.: MIX: a mosaic Asian anthropogenic emission inventory under the international  
1496 collaboration framework of the MICS-Asia and HTAP, *Atmos. Chem. Phys.*, 17, 935-963,  
1497 2017c.

1498 Li, M., Zhang, Q., Streets, D. G., He, K. B., Cheng, Y. F., Emmons, L. K., Huo, H., Kang, S. C.,  
1499 Lu, Z., Shao, M., Su, H., Yu, X., and Zhang, Y.: Mapping Asian anthropogenic emissions of  
1500 non-methane volatile organic compounds to multiple chemical mechanisms, *Atmos. Chem.*  
1501 *Phys.*, 14, 5617-5638, 2014.

1502 Li, M., Zhang, Q., Zheng, B., Tong, D., Lei, Y., Liu, F., Hong, C., Kang, S., Yan, L., Zhang, Y.,  
1503 Bo, Y., Su, H., Cheng, Y., and He, K.: Persistent growth of anthropogenic non-methane volatile  
1504 organic compound (NMVOC) emissions in China during 1990–2017: drivers, speciation and  
1505 ozone formation potential, *Atmos. Chem. Phys.*, 19, 8897-8913, 2019b.

1506 Liu, F., Zhang, Q., Tong, D., Zheng, B., Li, M., Huo, H., and He, K. B.: High-resolution  
1507 inventory of technologies, activities, and emissions of coal-fired power plants in China from  
1508 1990 to 2010, *Atmos. Chem. Phys.*, 15, 13299-13317, 2015.

1509 Liu, F., Zhang, Q., van der A, R. J., Zheng, B., Tong, D., Yan, L., Zheng, Y., and He, K.: Recent  
1510 reduction in NO<sub>x</sub> emissions over China: synthesis of satellite observations and emission  
1511 inventories, *Environmental Research Letters*, 11, 114002, 2016.

1512 Lu, Z. and Streets, D. G.: Increase in NO<sub>x</sub> Emissions from Indian Thermal Power Plants during  
1513 1996–2010: Unit-Based Inventories and Multisatellite Observations, *Environmental Science &*  
1514 *Technology*, 46, 7463-7470, 2012.

1515 Lu, Z., Zhang, Q., and Streets, D. G.: Sulfur dioxide and primary carbonaceous aerosol  
1516 emissions in China and India, 1996–2010, *Atmos. Chem. Phys.*, 11, 9839-9864, 2011.

1517 McDuffie, E. E., Smith, S. J., O'Rourke, P., Tibrewal, K., Venkataraman, C., Marais, E. A.,  
1518 Zheng, B., Crippa, M., Brauer, M., and Martin, R. V.: A global anthropogenic emission  
1519 inventory of atmospheric pollutants from sector- and fuel-specific sources (1970–2017): an  
1520 application of the Community Emissions Data System (CEDS), *Earth Syst. Sci. Data*, 12, 3413-  
1521 3442, 2020.

1522 Miyazaki, K., Eskes, H., Sudo, K., Boersma, K. F., Bowman, K., and Kanaya, Y.: Decadal  
1523 changes in global surface NO<sub>x</sub> emissions from multi-constituent satellite data assimilation,  
1524 *Atmos. Chem. Phys.*, 17, 807-837, 2017.

1525 Mo, Z., Shao, M., and Lu, S.: Compilation of a source profile database for hydrocarbon and  
1526 OVOC emissions in China, *Atmospheric Environment*, 143, 209-217, 2016.

1527 Paliwal, U., Sharma, M., and Burkhart, J. F.: Monthly and spatially resolved black carbon  
1528 emission inventory of India: uncertainty analysis, *Atmos. Chem. Phys.*, 16, 12457-12476, 2016.

1529 Phillips, D.: Ambient Air Quality Synergies with a 2050 Carbon Neutrality Pathway in South  
1530 Korea, *Climate*, 10, 1, 2022.

1531 Qu, Z., Henze, D. K., Li, C., Theys, N., Wang, Y., Wang, J., Wang, W., Han, J., Shim, C.,  
1532 Dickerson, R. R., and Ren, X.: SO<sub>2</sub> Emission Estimates Using OMI SO<sub>2</sub> Retrievals for 2005–  
1533 2017, *Journal of Geophysical Research: Atmospheres*, 124, 8336-8359, 2019.

- 1534 Saari, R. K., Selin, N. E., Rausch, S., and Thompson, T. M.: A self-consistent method to assess  
1535 air quality co-benefits from U.S. climate policies, *Journal of the Air & Waste Management*  
1536 *Association*, 65, 74-89, 2015.
- 1537 Samset, B. H., Lund, M. T., Bollasina, M., Myhre, G., and Wilcox, L.: Emerging Asian aerosol  
1538 patterns, *Nature Geoscience*, 12, 582-584, 2019.
- 1539 Shan, Y., Huang, Q., Guan, D., and Hubacek, K.: China CO2 emission accounts 2016–2017,  
1540 *Scientific Data*, 7, 54, 2020.
- 1541 Shi, Y. and Yamaguchi, Y.: A high-resolution and multi-year emissions inventory for biomass  
1542 burning in Southeast Asia during 2001–2010, *Atmospheric Environment*, 98, 8-16, 2014.
- 1543 Shibata, Y. and Morikawa, T.: Review of the JCAP/JATOP Air Quality Model Study in Japan,  
1544 *Atmosphere*, 12, 943, 2021.
- 1545 Simon, H., Beck, L., Bhave, P. V., Divita, F., Hsu, Y., Luecken, D., Mobley, J. D., Pouliot, G.  
1546 A., Reff, A., Sarwar, G., and Strum, M.: The development and uses of EPA’s SPECIATE  
1547 database, *Atmospheric Pollution Research*, 1, 196-206, 2010.
- 1548 Song, Y., Liu, B., Miao, W., Chang, D., and Zhang, Y.: Spatiotemporal variation in  
1549 nonagricultural open fire emissions in China from 2000 to 2007, *Global Biogeochemical Cycles*,  
1550 23, 2009.
- 1551 Stavrakou, T., Müller, J.-F., Bauwens, M., and De Smedt, I.: Sources and Long-Term Trends of  
1552 Ozone Precursors to Asian Pollution. In: *Air Pollution in Eastern Asia: An Integrated*  
1553 *Perspective*, Bouarar, I., Wang, X., and Brasseur, G. P. (Eds.), Springer International Publishing,  
1554 Cham, 2017.
- 1555 Sun, W., Shao, M., Granier, C., Liu, Y., Ye, C. S., and Zheng, J. Y.: Long-Term Trends of  
1556 Anthropogenic SO<sub>2</sub>, NO<sub>x</sub>, CO, and NMVOCs Emissions in China, *Earth's Future*, 6, 1112-1133,  
1557 2018.
- 1558 Takahashi, M., Feng, Z., Mikhailova, T. A., Kalugina, O. V., Shergina, O. V., Afanasieva, L. V.,  
1559 Heng, R. K. J., Majid, N. M. A., and Sase, H.: Air pollution monitoring and tree and forest  
1560 decline in East Asia: A review, *Science of The Total Environment*, 742, 140288, 2020.
- 1561 Van Damme, M., Clarisse, L., Franco, B., Sutton, M. A., Erismann, J. W., Wichink Kruit, R., van  
1562 Zanten, M., Whitburn, S., Hadji-Lazarou, J., Hurtmans, D., Clerbaux, C., and Coheur, P.-F.:  
1563 Global, regional and national trends of atmospheric ammonia derived from a decadal (2008–  
1564 2018) satellite record, *Environmental Research Letters*, 16, 055017, 2021.
- 1565 van der A, R. J., Mijling, B., Ding, J., Koukouli, M. E., Liu, F., Li, Q., Mao, H., and Theys, N.:  
1566 Cleaning up the air: effectiveness of air quality policy for SO<sub>2</sub> and NO<sub>x</sub> emissions in China,  
1567 *Atmos. Chem. Phys.*, 17, 1775-1789, 2017.
- 1568 van der Werf, G. R., Randerson, J. T., Giglio, L., van Leeuwen, T. T., Chen, Y., Rogers, B. M.,  
1569 Mu, M., van Marle, M. J. E., Morton, D. C., Collatz, G. J., Yokelson, R. J., and Kasibhatla, P. S.:  
1570 Global fire emissions estimates during 1997–2016, *Earth Syst. Sci. Data*, 9, 697-720, 2017.



1571 von Schneidmesser, E. and Monks, P. S.: Air quality and climate – synergies and trade-offs,  
1572 *Environmental Science: Processes & Impacts*, 15, 1315-1325, 2013.

1573 Wong, C.-M., Vichit-Vadakan, N., Kan, H., and Qian, Z.: Public Health and Air Pollution in  
1574 Asia (PAPA): A Multicity Study of Short-Term Effects of Air Pollution on Mortality,  
1575 *Environmental Health Perspectives*, 116, 1195-1202, 2008.

1576 Woo, J.-H., Choi, K.-C., Kim, H. K., Baek, B. H., Jang, M., Eum, J.-H., Song, C. H., Ma, Y.-I.,  
1577 Sunwoo, Y., Chang, L.-S., and Yoo, S. H.: Development of an anthropogenic emissions  
1578 processing system for Asia using SMOKE, *Atmospheric Environment*, 58, 5-13, 2012.

1579 Xiao, Q., Li, M., Liu, H., Fu, M., Deng, F., Lv, Z., Man, H., Jin, X., Liu, S., and He, K.:  
1580 Characteristics of marine shipping emissions at berth: profiles for particulate matter and volatile  
1581 organic compounds, *Atmos. Chem. Phys.*, 18, 9527-9545, 2018.

1582 Xie, Y., Dai, H., Xu, X., Fujimori, S., Hasegawa, T., Yi, K., Masui, T., and Kurata, G.: Co-  
1583 benefits of climate mitigation on air quality and human health in Asian countries, *Environment*  
1584 *International*, 119, 309-318, 2018.

1585 Yin, L., Du, P., Zhang, M., Liu, M., Xu, T., and Song, Y.: Estimation of emissions from biomass  
1586 burning in China (2003–2017) based on MODIS fire radiative energy data, *Biogeosciences*, 16,  
1587 1629-1640, 2019.

1588 Yuan, B., Shao, M., Lu, S., and Wang, B.: Source profiles of volatile organic compounds  
1589 associated with solvent use in Beijing, China, *Atmospheric Environment*, 44, 1919-1926, 2010.

1590 Zhang, C., Liu, C., Hu, Q., Cai, Z., Su, W., Xia, C., Zhu, Y., Wang, S., and Liu, J.: Satellite UV-  
1591 Vis spectroscopy: implications for air quality trends and their driving forces in China during  
1592 2005–2017, *Light: Science & Applications*, 8, 100, 2019.

1593 Zhang, Q., Streets, D. G., Carmichael, G. R., He, K. B., Huo, H., Kannari, A., Klimont, Z., Park,  
1594 I. S., Reddy, S., Fu, J. S., Chen, D., Duan, L., Lei, Y., Wang, L. T., and Yao, Z. L.: Asian  
1595 emissions in 2006 for the NASA INTEX-B mission, *Atmos. Chem. Phys.*, 9, 5131-5153, 2009.

1596 Zhang, Y., Cooper, O. R., Gaudel, A., Thompson, A. M., Nédélec, P., Ogino, S.-Y., and West, J.  
1597 J.: Tropospheric ozone change from 1980 to 2010 dominated by equatorward redistribution  
1598 of emissions, *Nature Geoscience*, 9, 875-879, 2016.

1599 Zhang, Y., West, J. J., Emmons, L. K., Flemming, J., Jonson, J. E., Lund, M. T., Sekiya, T.,  
1600 Sudo, K., Gaudel, A., Chang, K.-L., Nédélec, P., and Thouret, V.: Contributions of World  
1601 Regions to the Global Tropospheric Ozone Burden Change From 1980 to 2010, *Geophysical*  
1602 *Research Letters*, 48, e2020GL089184, 2021.

1603 Zhao, Y., Nielsen, C. P., Lei, Y., McElroy, M. B., and Hao, J.: Quantifying the uncertainties of a  
1604 bottom-up emission inventory of anthropogenic atmospheric pollutants in China, *Atmos. Chem.*  
1605 *Phys.*, 11, 2295-2308, 2011.

1606 Zhao, Y., Nielsen, C. P., McElroy, M. B., Zhang, L., and Zhang, J.: CO emissions in China:  
1607 Uncertainties and implications of improved energy efficiency and emission control, *Atmospheric*  
1608 *Environment*, 49, 103-113, 2012.

1609 Zhao, Y., Zhang, J., and Nielsen, C. P.: The effects of recent control policies on trends in  
1610 emissions of anthropogenic atmospheric pollutants and CO<sub>2</sub> in China, *Atmos.*  
1611 *Chem. Phys.*, 13, 487-508, 2013.

1612 Zheng, B., Cheng, J., Geng, G., Wang, X., Li, M., Shi, Q., Qi, J., Lei, Y., Zhang, Q., and He, K.:  
1613 Mapping anthropogenic emissions in China at 1 km spatial resolution and its application in air  
1614 quality modeling, *Science Bulletin*, 66, 612-620, 2021.

1615 Zheng, B., Chevallier, F., Yin, Y., Ciais, P., Fortems-Cheiney, A., Deeter, M. N., Parker, R. J.,  
1616 Wang, Y., Worden, H. M., and Zhao, Y.: Global atmospheric carbon monoxide budget 2000–  
1617 2017 inferred from multi-species atmospheric inversions, *Earth Syst. Sci. Data*, 11, 1411-1436,  
1618 2019.

1619 Zheng, B., Huo, H., Zhang, Q., Yao, Z. L., Wang, X. T., Yang, X. F., Liu, H., and He, K. B.:  
1620 High-resolution mapping of vehicle emissions in China in 2008, *Atmos. Chem. Phys.*, 14, 9787-  
1621 9805, 2014.

1622 Zheng, B., Tong, D., Li, M., Liu, F., Hong, C., Geng, G., Li, H., Li, X., Peng, L., Qi, J., Yan, L.,  
1623 Zhang, Y., Zhao, H., Zheng, Y., He, K., and Zhang, Q.: Trends in China's anthropogenic  
1624 emissions since 2010 as the consequence of clean air actions, *Atmos. Chem. Phys.*, 18, 14095-  
1625 14111, 2018.

1626 Zhou, Y., Xing, X., Lang, J., Chen, D., Cheng, S., Wei, L., Wei, X., and Liu, C.: A  
1627 comprehensive biomass burning emission inventory with high spatial and temporal resolution in  
1628 China, *Atmos. Chem. Phys.*, 17, 2839-2864, 2017.

1629